Wetting and Drying of Compacted Soils Under Laterally Restrained Conditions

By

Vinayagamoorthy Sivakumar, BSc, MSc, DIC, PhD, DSc, PGCHET, FICE CEng. Email address: v.sivakumar@qub.ac.uk.

Affiliation: Reader, Queen University Belfast, BT7 1NN,UK

Thangarajah Jeyaraj, BSc, MSc, PhD. Email address: thangarajah.Jeyaraj@bam.com

Affiliation: Senior Engineer, Bam Nuttall Ltd St James House, Knoll Road, Camberly GU15 3XW

Pauline Mackinnon, BEng, PhD, CEng., MICE, CEng. Email address: p.mackinnon@qub.ac.uk

Affiliation: Senior Lecturer, Queen University Belfast, BT7 1NN,UK

Snehasis Tripathy, MEng, PhD. Email address: TripathyS@cardiff.ac.uk

Affiliation: Professor, Cardiff University, Cardiff CF10 3AT, UK

Revised article submitted to ASCE for possible publication.

Corresponding author

Vinayagamoorthy Sivakumar

School of Natural and Built Environment

David Keir Building

Queen's University Belfast

Belfast BT7 1NN

Email v.Sivakumar@qub.ac.uk

Wetting and Drying of Compacted Soils Under Laterally Restrained Conditions

ABSTRACT

Compacted soils are components of geo-infrastructure applications which are unsaturated at the time of placement. Their responses to climate change, in the form of prolonged summers and wet winters, can be complex. This article examines the evolution of horizontal stresses behind retaining structures backfilled with compacted soil during formation, through wet and dry cycles. Samples of Kaolin Clay and Belfast Clay were tested. The horizontal stresses during the formation of these compacted samples were examined initially and then the samples were subjected to wetting and drying cycles under horizontally restrained conditions.

For design purposes, there are many proposals, including assuming the coefficient of earth pressure $K_0^* \approx K_a^*$ compacted fills. However, the observations obtained on both clays have indicated clearly that the values of K_0^* can be below unity only at high overburden pressures. Further repeated wetting and drying of samples under constant overburden pressure resulted in a complex response. Belfast Clay exhibited a gradual increase in K_0^* with wetting cycles, but kaolin exhibited a noticeable reduction in the value of K_0^* upon first wetting. However, subsequent wetting followed by drying showed a significant recovery of the K_0^* value.

Practical applications

Compacted soils are commonly used in engineering constructions for a range of applications such as sub-base for roads, backfilling retaining structures, dams/dykes, and landfill liners. The compacted soils should be placed in accordance with “standards” available in the respective countries. However, their post placement behaviour is complex and influenced by several factors including climate change. Compacted soils can exhibit swelling upon wetting and the reverse (shrinkage) may prevail during drying. If such swelling or shrinkage is restricted, for example in the form rigid retaining structure, the contact pressure between the rigid structure and the soil can vary significantly during climatic events. This article endeavoured to address this issue from an experimental point of view, and the finding from the research highlighted some interesting observations on aspect of the pressure development in horizontal direction.

INTRODUCTION

In the unlikely event of a considerable reduction in greenhouse gas emissions, climate change will continue to take place, possibly for centuries to come (NOAA 2024), with the resulting impacts being seen as a threat to the resilience of critical infrastructure (IPCC 2023), including the geo-infrastructure upon which much of our transport and utilities infrastructure is built on or within. Geo-infrastructure has often failed to function under severe climatic conditions (Toll *et al.*,2012; Loveridge *et al.*,2010; Smethurst *et al.*,2015) and extreme weather events have already caused numerous geotechnical disasters (Giles and Griffiths 2020), with countries with temperate climates spending billions of pounds on repair works (Rising *et al.*, 2022). Some of the common geo-infrastructures are slopes, dikes, retaining walls, buried storage facilities and water/gas pipeline-networks. The effects of climate on geo-infrastructures are undeniable, and the resulting impacts are often severe and unpredictable in many ways. This article deals with a specific problem relating to the assessment of the potential impact of climate change on rigid retaining walls back-filled with clay-based geo-materials.

The way in which back-fill materials respond to climate change and the consequent impact on retaining structures is complex. The preferred back-fill materials are typically granular, and this choice is based on the inert nature and inherent suitability for withstanding climatic events. With sustainability being the number one priority in the construction industry, one should look for site-won materials as potential back-fill materials. Such soil deposits can be clay-rich, depending on the geographical locations. Guidelines exist for the use of clay-based materials (Design Manual for Roads and Bridges, Highways Agency, 1995; Specification for Highway Works, Highways Agency, 2004), however, engineers conservatively choose granular fill materials to avoid any potential issues or adverse effects arising. On any given construction project, clay-based natural materials/subsoils are a common occurrence and embedded forms of retaining structures, such as secant piled walls will invariably retain or interact with these types of deposits. Under restrained conditions, clay-based materials can produce large horizontal pressures upon wetting (Clayton *et al.*, 1991). However, the use of clay fills should be promoted to reduce: (a) the sustained extraction of granular materials, (b) help promote the preservation of green-belts, and (c) lower emissions of CO_2 into the atmosphere (resulting from extraction and transportation/importation of granular/engineered fill. Accordingly, practicing engineers require adequate guidance on the use of clay-based materials for construction purposes.

With appropriate construction technologies, clay-based materials can be considered for a variety of applications. However, one should understand how unsaturated compacted or natural clay-based materials perform under restrained conditions, such as behind retaining walls or as a composite element in other forms of retaining structures. For instance, consider an element of compacted clay behind a retaining structure (Figure 1a). Immediately after the compaction the soil is unsaturated, but subsequent rainfall may increase the water content, resulting in swelling (discussed in the next section). If that swelling takes place under horizontally restrained conditions, the pressure acting on the retaining wall will increase (Sivakumar *et al.,* 2016). During drying there can be an ease of pressure, leading to the formation of tension cracks (Figure 1b). If these events are continued in the long- term, the stability of the retaining wall will be in question (Mawditt *et al*., 1989). These aspects were investigated through a series of testing programmes using Belfast Clay and Kaolin Clay. It is not the intention of this work to investigate how pressure development can be reduced or delayed, but this can be the subject of future research. At this stage, it may be worthwhile to highlight some of the basic understanding of unsaturated compacted clay behaviors.

Behavior of unsaturated soils:

Compacted fills are usually placed at about the optimum water content (OWC), as measured from standard Proctor compaction tests (Proctor,1933), and they are often in an unsaturated state. It is widely accepted that the traditional effective stress equation ($\sigma' = \sigma - u_w$, where σ', σ and u_w are the total stress, effective stress and pore water pressure respectively) cannot be used to model unsaturated soil's behavior. In an attempt to resolve this issue, various proposals have been made in the last five decades and the approach that still thrives as a plausible and widely used alternative is the "two-stress-state" variables (Fredlund *at al.,* 1978) given by $(\sigma - u_a)$ and $(u_a - u_w)$ where u_a is the pore air pressure and the difference between u_a and u_w is referred to as suction, s. The authors accept that the other forms of stress variables, often referred to as "control stress" or coupled-stress" (Murray *et al*., 2010), do function reasonably well under specific conditions. However, within the remit of the current investigations, "two-stress-state" variables are considered to be appropriate.

The volumetric response of unsaturated compacted clays upon wetting has been investigated by many researchers (Alonso *et al*., 1990; Wheeler and Sivakumar, 1995; Cui *et al*., 1996; Lloret *at al*., 2003; Lu *et al*., 2004; Sivakumar *et al*., 2010). The framework is based on:

$$\bar{p} = \frac{\bar{\sigma}_1 + 2\bar{\sigma}_3}{3}$$

$$q = \bar{\sigma}_1 - \bar{\sigma}_3$$

$$s = u_a - u_w$$

$$v = 1 + e$$

$$v_w = 1 + e_w$$

where $\bar{p}$, q, v, e, v_w and e_w are mean net stress, deviator stress, specific volume, void ratio, specific water volume and water void ratio respectively. One of the key attributes of the work mentioned by the above researchers was the loading-collapse mechanism of unsaturated soils, represented by the yield domain presented in Figure 2a. Let us consider the initial state of the soil is at Point A and then taken through a Path ABC, which involves reduction in suction (or wetting). Compacted soils often possess bi-modal pore structure in which individual particles group together forming "aggregates" which are separated by "macro voids". The voids within the aggregates are referred to as "micro voids" (Figure 3). Upon reduction in suction, the individual aggregates will swell, but at the same time, there can be aggregate slippage due to insufficient shear resistance at the aggregate contact points (Figure 2b). The overall behaviour is dependent on the intensity of the above two components. In lightly compacted soil, the aggregate slippage could become more predominate during wetting (as represented by Point B onwards in Figure 2a) and the remaining wetting path BC will exhibit collapse settlement (illustrated in Figure 2c). However, in heavily compacted soil (where the yield domain will be large and as indicated in Figure 2a), the aggregate slippage may not be significant and, therefore, the entire wetting path may exhibit swelling (as depicted by the red line curve in Figure 2c). There are other crucial aspects of unsaturated soils behaviour that need to be elucidated, but these will be explained at the appropriate juncture in the remaining part of the article.

The key aspect under the investigation is the coefficient of earth pressure at rest in unsaturated soils. In saturated soils, the coefficient of earth pressure K_o is defined as the ratio between the horizontal and vertical effective stresses "at rest" (no horizontal straining). This definition is extended to unsaturated soils in terms of net stresses (Sivakumar *et al*., 2015):

$$K_o^* = \frac{\sigma_h - u_a}{\sigma_v - u_a} = \frac{\bar{\sigma}_h}{\bar{\sigma}_v}$$

where σ_v, σ_h, and u_a are respectively the total vertical stress, total horizontal stress and pore air pressure. The symbol K_o^* is used to differentiate it from the coefficient of earth pressure of saturated soils, K_o. The parameter K_o^* can be used to examine the stress development on the retaining structure during wetting and drying events.

EXPERIMENTAL PROGRAMME

Soil type

Kaolin Clay (KC) and Belfast Clay (BC) were selected for the proposed testing programme. KC is available in dry powdered form and the specification of the clay used in the research is "speswhite kaolin". This clay has a clay content of approximately 85%, with the remaining 15% being fine silts; however, these latter constituents also comprised mainly kaolinite minerals. The Liquid and Plastic Limits of KC were 70% and 31% respectively and, therefore, it is classified as a very high plasticity clay. Belfast Clay (BC) underlies large areas of the Belfast geological basin (Doran, 1992) and it was extracted in disturbed form from an excavation site. The predominant clay minerals were muscovite (32.5%) and Dolomite (16.3%) and other minerals. The respective clay, silt and sand fractions were about 38%, 57% and 5%. The Liquid and Plastic Limits were approximately 56% and 27%, respectively. The material is classified as an intermediate plasticity CLAY (Table 1).

Standard Proctor compaction characteristic

Pre-processing was not required in the case of KC as it was available in powder form. In the case of BC, the natural materials were oven dried for 24 hours at 105^{o}C and crushed into small particles, smaller than

3.3 mm in size. Water was added to 3 kg of the sieved soils to achieve a target water content, and they were stored in a sealed plastic bag for 24 hours to achieve a reasonably uniform water content. The compaction process was carried out at 5 different water contents. The Standard Proctor compaction (BS1377-4-1990 analogous to ASTM D1557) involved: compaction in three layers by dropping a 2.5 kg hammer 25 times through 300 mm. The information required for this research was optimum water (OWC) content and maximum dry density (MDD), and the values for KC and BC are listed in Table 1.

Experimental System

Formation of compacted sample: In an ideal situation, the samples should have been produced by dynamic compaction, as described in BS1377-4-1990 or ASTM D1557. However, this approach was considered not feasible or unsuitable for two reasons: (a) there is no equivalent standard procedure for compacting samples in a mould having 50 mm diameter (i.e., proposed sample diameter), and (b) there can be some variability of initial conditions within and among samples. Therefore, a decision was taken to produce samples using static compression (by means of compressing the soil to elevated pressures) in such a manner as to attain similar (or closer) MDD at the OWC, as that of the standard procedure. Wheeler and Sivakumar, 1995 and Sivakumar *et.al.,* 2010 have demonstrated excellent repeatability of producing samples using this method. In addition, the current investigation also required the assessment of horizontal stresses during the process of compression. To achieve this, initial trials were carried out to compress the soil in a rigid one-dimensional mould instrumented with pressure cell in horizontal direction. However, the pressure measurements in the horizontal direction proved to be unreliable, largely due to significant friction between the soil and the wall of the rigid mould. It was therefore decided to compress the soil under flexible horizontal boundary conditions with provision to restrain the soil from deforming horizontally and the procedure adopted is described below.

The experimental system used for the above purpose is graphically illustrated in Figure 4a. It consisted of:

- A high capacity tensiometer on the pedestal to measure suction during the formation of the sample to a required bulk or dry density under a constant water mass condition. The tensiometer has a capacity of measuring suction up to 1500 kPa. The procedure adopted to saturate the tensiometer is reported by Lynch *et al*. (2019).
- An internal (radial) strain gauge to accurately measure and control horizontal strain. The purpose of this was to mimic one-dimensional compression, i.e., restraining the sample from horizontal expansion or contraction using a control program "TRIAX" (Toll, 1999) - to elevate or reduce the horizontal pressure acting on it. During this process, the tolerance of horizontal strain was kept within a small range (±0.004%), where the sample diameter was 50 mm.
- A facility to apply tension loading (or otherwise negative deviator stress, q) if needed using a hook arrangement and as shown in Figure 4a. During compression, vertical pressure will be higher than the horizontal pressure under horizontally restrained conditions. During unloading under similar restrained

conditions, the horizontal pressure can become higher than the vertical pressure, implying a negative deviator stress q, and the hook arrangement referred to above facilitating or allowing this action to occur.

- A stainless-steel chamber to enclose the sample and apply confining pressure to the soil sample. This allowed more accurate measurement of water volume entering or leaving the chamber, triggered by reduction or increase in sample volume respectively. The chamber was initially calibrated for apparent volume change, thus allowing the sample volume change to be calculated with reasonable accuracy (Sivakumar *et al.*, 2010).
- Axial load to the sample was applied by increasing the lower chamber pressure as indicated in Figure 4a. The pressure in the lower chamber was controlled using a constant rate pump. The axial strain of the sample was measured externally to the system.

A known amount of clay was mixed with water to achieve a predetermined water content (i.e. close to the relevant OWC). A cylindrical split-mold, 50 mm in diameter, was used to form a very loose sample that could hold together at least during the setting-up procedure. About 50g of mixed material was poured into the mold and a plug, 49.5 mm in diameter, was placed at the top of the material. A static load of 10 kg was placed on the plug (equivalent to 50 kPa) and left for 2 minutes. The load and the plug were removed, and the top surface of the lightly compressed material was scarified. A further 50g of material was added and the above procedure was repeated for a total of 8 layers. Finally, the split mould was opened to remove the very loose sample, and it was trimmed to a height of 70 mm (Figure 4b).

The sample was covered in a rubber membrane. The top cap (combined with a hook) was then located on the sample. The membrane was sealed on the pedestal and top cap. Note here that the drainage of air and water was not allowed during compression. Upon completion of setting up the sample, the stainless-steel chamber was assembled and fastened. The chamber was then filled with de-aired water. The loading ram - with a key at the end - was then carefully inserted through the hole in the chamber and it was then engaged with the hook. The system was then located on the loading frame. The top of the loading ram was threaded so that it could be screwed on to the load cell. This action needed careful maneuvering as any tension or compression loading could damage the loose sample. To avoid any pitfalls, the holding frame for the load cell was relaxed so that it could move up or down freely during the operation. An initial confining pressure of 15 - 20 kPa was applied as a reference pressure. Horizontal strain, axial strain and load were re-set to zero. The vertical pressure was then applied at a rate of 20 kPa per hour. As one would expect, the axial compression could result in horizontal expansion of the sample. TRIAX control program ensured the horizontal strain remained zero (or within the stipulated range) by increasing the cell pressure. The loading lasted about 3 days, and it was terminated when the bulk density of the sample reached approximately the value obtained from Proctor compaction at the respective water contents (any further application of pressure will make the samples over-compressed and densities being higher than otherwise obtained using the standard compaction practice). Note also, this procedure required regular observations and interpretations on a time-line basis to avoid over-pressuring the samples. This was then followed by the unloading process. Again, the control program ensured a horizontally restrained condition and the vertical pressure on the sample was reduced to as low as 15 kPa.

Testing programme under wetting and drying cycles

The samples of KC and BC were subjected to wetting and drying cycles. The suction in the samples was controlled using the axis translation technique (Hilf, 1956). The high air entry filter used in this investigation has a capacity of 1500 kPa, which was saturated using a procedure described by Sivakumar *et. al.*, 2010. The horizontal strain gauge was located at mid-height of the sample (Figure 5). It was followed by the placement of the top cap (included with a hook arrangement for applying tension loading). This top cap also incorporated the air supply line to apply pore air pressure u_a. A pair of inclinometers were located along the sample for measuring axial strains. The top plate of the stress path cell was carefuly assembled and this required methodological manoeuvring when locating the key on the top cap. The cell was filled with water and pressurised to 25 kPa as a reference pressure.

The initial conditions of the sample for KC and BC are tabulated in Table 2. For example, for KC at 10 m depth, the initial conditions were: vertical net pressure 200 kPa, horizontal net pressure 225 kPa, and suction 475 kPa. These values were extracted from the information collected during the formation of the compacted soils (discussed later in more detail). To achieve these stress conditions, the cell pressure σ_3, air pressure u_a and water pessure u_w, were slowly increased or to 750 kPa, 525kPa, 50 kPa while the axial load was reduced to -49N (equivalent to -25 kPa of deviator stress q) respectively. The negative vertical load implies that the deviator stress was in the negative range to meet the initial condition of K_o^*=1.125 (i.e., horozontal pressure was higher than the vertical pressure). The sample was allowed to equlibriate at this condition for 3 to 4 days until there was no water movement into or out of the sample. In the subsequent testing, the suction in the sample was reduced by elevating the pore water pressure u_w. The stages through which the suction was reduced are tabulated in Table 3. Upon reaching a suction of 100 kPa (as stipulated in Table 3), the samples were dried by increasing suction. This could have been carried-out in two ways: (a) by reducing the pore water pressure u_w or (b) increasing the pore air pressure u_a. Both approaches posed some risks: (a) reducing the pore water u_w pressure could trigger cavitation of water in the drainage lines, ie., the water that was exposed to high air presure within the sample leaving the soil via the high air entry filter to reach the volume change unit can trigger air coming out of solution and potentially null-functioning the filter disc and (b) increasing the air pressure u_a also requires cell pressure σ_3 to be increased at the same time by the same magnitude to avoid a jump in the net horizontal and vertical pressures. In the current investigation, the second approach was adopted. This procedure was implemented until a target suction value was achieved, as shown in Table 3. Upon reaching the end of the drying stage, the sample was rewetted by elevating the pore water pressure in a similar fashion to that described above. The approach adopted also allowed only limted wetting and drying cycles as the maximum air pressure in the laboratory was 800 kPa (apart from the fact that the cell pressure was increased beyound this limit using a hydraulic multipler, that was not possible with pore air pressure u_a).

RESULTS AND DISCUSSION

Formation of compacted fills. Pressure evolutions during static compression were assessed on both KC and BC. The targeted water contents of these samples were slightly lower than the OWC achieved using BS1377-4-1990/ASTM D1557 by 1.2% and 1.9% for KC and BC respectively. Therefore, on that note, the targeted bulk/dry densities refer to those respective water contents on the Proctor compaction characteristics.

Kaolin Clay: Figure 6a shows the evolution of net vertical and horizontal pressures during the one-dimensional loading and unloading under horizontally restrained conditions. The loose sample was initially subjected to 25 kPa of equal pressure all around the sample. Hence, at the beginning of the loading, σ_v- u_a = σ_h- u_a. The net vertical pressure was then increased to 1,300 kPa at a slow rate (Loading Path ABCD) and then reduced to around 25 kPa during unloading (Path DEFG). The maximum loading of 1,300 kPa represents the sample reaching a bulk density that was comparable to the bulk density obtained from Standard Proctor compaction at the same water content (i.e., it was slightly lower than the OWC). Figure 6b shows the evolution of suction in the sample during the process of loading and unloading. The suction at the beginning of loading was approximately 500 kPa and it reduced to 100 kPa at the peak of the loading. Upon unloading, the suction increased to 550 kPa (Point G), about 50 kPa more than the suction measured at the beginning of compression (i.e. at Point A). The development of suction during the loading and unloading process can be explored further using Skempton's pore water pressure parameter B (Skempton, 1964) and attributing reasons for the apparent increase in suction during unloading. However, it cannot be conveyed adequately within the length constraints of this article. The specific volume reduced from an initial value of 2.82 to 1.90 at the peak of the loading (Figure 6c, where X axis refers to the net vertical pressure). It appears that the sample possibly yielded at about 50 kPa, much like the pressure applied during the initial formation of the sample in a split mould. The degree of saturation progressively increased from its initial value of 34% to about 80% at maximum loading (see Figure 6d.). This degree of saturation is approximately the same as the value obtained from Proctor Compaction.

At the early stage of the loading process the value of K_0^* was 0.44 (represented by the broken line passing Point A) and gradually increased to 0.66 at maximum loading. At the termination of loading (25 kPa of vertical pressure), the value of K_0^* was approximately 4.0. The horizontal pressure in compacted fills will vary from top to bottom depending on the depth (discussed later in this article). The locations considered in the current investigations refer to "shallow" depth at 2.5 m and "deep" depth at 10.0 m from the ground surface behind the retaining wall (Figure 1). The condition after placement of the fill at 10.0 m depth is represented by X in Figure 6a. At this condition the value of K_0^* is approximately 1.125. At a depth of 2.5 m, the value of K_0^* is approximately 2.3 (represented by Point Y in Figure 6a). These values are calculated assuming the unit weight of the fill was 20 kN/m^3.

Belfast Clay: Figure 7a shows the evolution of net horizontal pressure during the loading and unloading process. The net vertical pressure (σ_v- u_a) was increased from 25 kPa to 1,427 kPa (Path ABCD; 1427 kPa represents the pressure required to achieve bulk density - like that obtained from Standard Proctor compaction at the respective water content) and then reduced to 15 kPa (Path DEFG). Figure 7b shows the development of suction in the sample during the process of compression. Suction in the sample at the beginning of loading was approximately 420 kPa and it reduced to -250 kPa (i.e. positive pore water pressure) at the peak of the loading. Upon unloading, the suction increased to 444 kPa and about 24 kPa more than the suction measured at the beginning of the compression (refer to comments made on KC). The specific volume reduced from an initial value of 2.547 to 1.730 at the peak of the loading (Figure 7c, where X axis refers to the net vertical pressure). The sample possibly yielded at about 50 kPa, similar to the pressure applied during the initial formation of the sample in split- mould. The degree of saturation progressively increased from its initial value of 36% to about 80% at maximum loading (see Figure 7d) and this value is comparable to the value obtained from Proctor compaction.

The value of K_0^* at the beginning of the loading is about 0.40 (represented by the broken line passing through Point A) and gradually increased to 0.73 at the termination of the loading. At the termination of loading, the value of K_0^* was approximately 6.5. The condition after placement of the fill at 10.0 m depth is represented by X in Figure 7a. At this condition the value of K_0^* is approximately 1.25. At a depth of 2.5 m, the value of K_0^* is approximately 3.0, represented by Point Y in Figure 7a.

Horizontal earth pressure during compaction, particularly against a restrained structure is of great interest among researchers, which has attracted numerical and field-based investigations over several decades. Ingold, 1979; Duncan *et al,* 1991; Simons and Clayton 1992; Filtz and Duncan, 1996; Han *et al,* 2024. There have been several proposals, including some propositions stating that the horizontal pressure would reach closer to active pressure, but, on other hand, some suggest that its value could be as high as 25-30% of undrained shear strength. Although the present investigations assessed its magnitude (in terms of K_0^*) using laboratory-based investigations, the findings are comparable to one of the recent investigations reported by Han *et al.,* 2024. Figure 8 shows the profiles of K_0^* with depth for KC and BC, based on the information shown in Figures 6 and 7. The values of K_0^* are much higher than one after placement up to a depth of about 15m. This depth corresponds to deep retaining structures. Certainly, the K_0^* values at shallow depths are close to passive earth pressure coefficient K_p, as defined for saturated soils (in agreement with Han *et al.,* 2024). Considering another perspective, between these two clays, BC is an intermediate plasticity clay. It contained a small amount of sand, with the remaining constituents being silt and clay. The values of K_0^* at significant depths appear to be similar between the two soils, however, their values vary considerably at shallow depths. At shallow depths (for example 1.0 m below the ground surface), KC yielded a K_0^* value of 3.6, whereas for BC, it was 6.5. Both clays were compressed to achieve maximum densities like those obtained using BS compaction at the respective water contents. Therefore, the compaction effort cannot be regarded as a contributing factor for the apparent disparity in the K_0^* values at shallow depths. Other possible factors to consider are the effective angle of friction ϕ' (KC 21^0; and BC 28^0, Sivakumar *et al.,* 2009 and 2017) and deviation of compaction water contents from the optimum water content (KC: 1.2%, OWC = 29% on dry side BC: 1.9% OWC = 23% on dry side) and the potential influence of bi-modal pore structure that compacted soils often have. Based on the effective angle of internal friction, it could be expected that KC would exhibit much higher K_0^* than BC. While the deviation of compaction water content from its optimum value for each soil can be a potential reason for disparity in the K_0^* values at shallow depths, the influence of the bi-modal pore structure on the earth pressure coefficient cannot be ignored. Sivakumar *et al*. (2010a) reported that stress-induced anisotropy has a profound influence on the pressure-volume relationship of unsaturated soils and, indeed, further observations were also made in the subsequent investigations (described below) to justify the apparent differences in K_0^* values between the two clay specimens.

Evolution of stresses upon wetting and drying

Table 3 lists the stages used in taking the samples through the wetting-drying-wetting cycles. Also, the initial conditions of the samples prior to the wetting and drying cycles are illustrated in Figure 9. In the case of BC at 50 kPa of overburden pressure, the vertical ($\overline{\sigma_v}$), horizontal ($\overline{\sigma_h}$) and suction (s) stresses were 50, 150, 400 kPa respectively, representing a K_0^* value of 3.0. To achieve these pressures, cell pressure *(σ_3)*, air pressure (u_a) and water pressure u_w of 600 kPa, 450 kPa and 50 kPa respectively were applied. To achieve a K_0^* of 3.0, the vertical pressure was reduced by applying a negative loading of -196N (equivalent to -100 kPa). The investigation commenced with the first wetting referred to as S_1: first drying D_1: and second wetting, S_2. The samples were allowed to equalize at each suction value (either during wetting or drying) and this condition was indicated by no significant movement of water into or out of the sample at the end of the equalization process. Each stage lasted about 5 days. The aspects explored in the interpretation of the data are specific volume *v*, axial strain ε_a, degree of saturation S_r, stress path in *q: s* and K_0^*.

Belfast Clay (at shallow depth): Figure 10 shows the variations of *v*, ε_a and S_r with suction during the wetting and drying stages under $\overline{\sigma_v}$ = 50 kPa. At the start of the wetting process, *v*, S_r and s were 1.662, 84.8% and 400 kPa respectively. The wetting process was terminated at a suction value of 100 kPa, during which *v* increased to 1.684, S_r reached a value of 89.1% and the axial strain ε_a at this stage was approximately 1.31% (swelling). The drying process would trigger a reduction in volume, resulting from axial and horizontal contractions. As horizontal strain was not permitted, the system therefore would trigger a reduction in horizontal pressure to meet the relevant boundary conditions. However, the minimum horizontal pressure that can be applied using a stepper motor-driven pressure regulator was 5 kPa. Therefore, the drying process was terminated when there were some indications of horizontal strains exceeding the safe band set in the control program, monitoring the performance of the soil. At this point s, v, S_r and ε_a were respectively recorded at 500 kPa, 1.670, 87.7% and 0.51% (net axial compression of 0.80%). The second wetting process began at S_{21} and at the end of the second wetting process (S_{22}) s, v, S_r and ε_a were 100 kPa, 1.692, 91.5% and 1.78% respectively. Due to limitations in the pressure supply available in the laboratory, the test was terminated after the second wetting and no further drying stage was undertaken.

There are many important observations made from the test described above. Both wetting processes ended with a suction value of 100 kPa. The second wetting process increased the specific volume marginally, however, there was not enough data to confirm if further repeated wetting and drying processes would progressively increase the specific volume. During the drying process zero horizontal strain conditions began to exceed the set-limit at a suction value between 400 kPa and 500 kPa, but the exact value is not known since the suction was increased in an incremental fashion. Although the horizontal strain exceeded the set-limit violated at suction value of 500 kPa, its magnitude was approximately -0.008% (contraction) - equivalent to contraction of 0.004 mm in 50 mm diameter sample). Upon the second wetting, the suction value was reduced to 100 kPa. At the end of the second wetting, the relevant volumetric variables (v, ε_a and S_r) were higher than those observed during the first wetting. In essence, the wetting and drying process resulted in a marginal increase in the volumetric variables, but it is not possible to confirm that these parameters continue to increase with repeated wetting and drying cycles as this investigation was limited to a relatively small number of wetting and drying cycles.

Figure 11 shows the deviator stress and K_0^* variation with suction during the wetting and drying processes. At the beginning of the first wetting, the deviator stress q was -100 kPa, implying that the sample was under tension loading. The initial K_0^* was 3.0. During the wetting process the deviator stress reduced to -155 kPa and at this point $K_0^* \approx 4.2$. Referring to Figure 10a, specifically during the first wetting, the specific volume increased by 0.022 and the sample swelled axially by 1.31% (Figure 10b). These observations agree with the changes in the pressure regime, where the deviator stress q reduced by about 55 kPa to keep the horizontal strain conditions within the stipulated limits.

During drying, the sample contracted axially by 0.8% (from its previous state), leaving it with a permanent axial swelling of about 0.50%, at which the suction was 500 kPa. As expected, the horizontal stresses reduced significantly to maintain zero horizontal strain conditions. This made the deviator stress change from tension loading to compressive loading (i.e. -155 kPa to +48 kPa). At this point, the value of $K_0^* \approx 0.1$. It should be noted that the testing system was not capable of applying net horizontal pressure less than 5 kPa, and any small change in horizontal stress would result in a significant change in K_0^*. During the second wetting, the deviator stress reduced from +48 kPa to -155 kPa, corresponding to $K_0^* \approx 4.2$ at the end of the wetting. This value is almost the same as the value attained during the first wetting, though the second wetting process exhibited significantly more swelling (refer to Figure 10a).

Belfast Clay (at deep depth): Figure 12 shows the variations in v, ε_a and S_r during the wetting and drying processes under $\overline{\sigma_v}$ of 200 kPa. Their initial values were 1.659, 0.0% and 82.9% respectively. The first wetting process was terminated at a suction value of 100 kPa, at which the respective values of v, S_r, ε_a increased to 1.668, 87.1% and 0.52% (swelling). The axial strain in this case was significantly lower than the axial strain observed when the sample was wetted at $\overline{\sigma_v}$ = 50 kPa. The reason for this will be discussed in the assessment section, later in this article. The drying process was terminated at a suction value of 600 kPa, and there were no indications of tension cracks (violation of horizontal strain conditions). The values of v, S_r and ε_a at the end of the drying stage were 1.660, 85.4% and 0.04% respectively (with the sample contacting by 0.48% from the start of the drying state). At the end of the second wetting, the values of v, S_r and ε_a were 1.669, 89.0% and 0.60% respectively.

Both wetting stages were terminated at a suction value of about 100 kPa. The repeated wetting resulted in a progressive increase in v, ε_a and S_r. This observation is like that observed in the case of the sample tested under $\overline{\sigma_v}$ = 50 kPa. The one-off drying process also resulted in an increase in all three volumetric variables compared to the initial values. Horizontal strain did not violate the set conditions, even at a suction value of 600 kPa. However, in the earlier test (Test No: BC-S3-50, $\overline{\sigma_v}$ = 50 kPa), violation was observed at 400-500 kPa. Accordingly, it can be suggested that the formation of tension cracks depends on the stress level in the ground. The term tension cracks here implies that the horizontal pressure approaches near zero (accordingly K_0^*). Since the samples were enclosed in rubber membrane such phenomena could not be substantiated via other means.

Figure 13 shows the deviator stress and K_0^* variation with suction during the wetting and drying processes. At the beginning of the first wetting, the deviator stress q was -51 kPa, implying that the sample was under tension loading. During the wetting process the deviator stress reduced to -143 kPa, and at this point the K_0^* value increased to 1.69. Referring to Figure 12, during the first wetting, the specific volume increased by 0.009 and the sample swelled axially by 0.52%. This value is significantly less than the axial swelling observed in the test, where the overburden pressure was 50 kPa (shallow depth) and the relevant axial strain was 1.31%. The reason for the reduced swelling under high stress level is discussed later, in the assessment section of the text. During the drying process, the value of $K_0^* \approx 0.2$ at s = 600 kPa. The subsequent wetting resulted in a recovery of K_0^*, reaching a value that was observed during the first wetting phase.

Kaolin Clay (at shallow depth): Figure 14 shows the relevant volumetric variables varying with suction during the wetting and drying processes. During the wetting process the values of v, S_r and ε_a increased to 1.969, 88.4% and 2.0% respectively. At the end of the drying process, the respective values of v, S_r and ε_a were 1.952, 81.3% and 1.1% (net swelling). The suction value at which the horizontal strain began to exceed was in the range between 375 kPa and 425 kPa. Therefore, the drying process was terminated at a suction value of 425 kPa. The second wetting continued until a suction value of 20 kPa and, at this suction, the values of v, S_r and ε_a were 1.979, 93.0% and 2.5% (net swelling) respectively. Figure 15 shows the deviator stress and K_0^* variation with suction. At the beginning of the first wetting phase, the deviator stress q was -65 kPa, corresponding with a value of K_0^* = 2.30. During the wetting process the deviator stress increased to -40 kPa, and at this point, $K_0^* \approx$ 1.92. This behavior is contradictory to the observations made in the case of Belfast Clay under the same overburden pressure (i.e. $\overline{\sigma_v}$ = 50 kPa), where the deviator stress reduced (or K_0^* increased to keep the zero horizontal strain conditions). At odds with this, the increase in specific volume and axial strain during the first wetting process would only imply that the sample wanted to swell also in the horizontal direction and was restrained to meet the testing conditions (zero horizontal strain) by increasing the horizontal stresses. However, the opposite action, i.e. reduction in horizontal stress prevailed during the first wetting. Hence, an interesting situation appears to have emerged, where the initial wetting process may have resulted in contraction of the sample in the horizontal direction and a significant amount of swelling in the axial direction. This observation requires an explanation which is provided in the assessment section.

During the drying process, the sample contracted axially by 0.9% (from its previous state), leaving a permanent axial swelling of about 1.2% at which the suction was 400 kPa. The horizontal stress reduced significantly to maintain zero horizontal strain conditions. This made the deviator stress change from tension loading to compressive loading. At this point, the value of $K_0^* \approx$ 0.05. During the second wetting stage, K_0^* recovered and reached a value of $\approx$ 1.98 at a suction value of 20 kPa, significantly lower than the initial K_0^* value.

Kaolin Clay-(at deep depth): Figure 16 shows the variations of v, ε_a and S_r with suction. The initial values of v and S_r were 1.938 and 77.2% respectively. The first wetting process was terminated at a suction value of 100 kPa and, at this point, the values of v, S_r and ε_a increased to 1.964, 89.8% and 1.31% respectively. The axial strain was significantly lower than that observed when the sample was initially wetted under a vertical stress $\overline{\sigma_v}$ of 50 kPa. At the end of drying the respective values of v, S_r and ε_a were 1.946, 80.9% and 0.40% (axial compression by 0.91%), and the corresponding suction was 475 kPa. At this stage there was no violation of horizontal strain conditions. At the end of the second wetting process the values of v, S_r and ε_a were 1.972, 92.7% and 1.70% respectively, with suction of 20 kPa. Note that the suction at the end of first wetting was 100 kPa and, at the end of the second wetting period, was 20 kPa. At the end of the second wetting, the specific volume, degree of saturation and axial strain were higher than those at the end of the first wetting but, corroborating these parameters at a suction of 100 kPa, it appears that the repeated wetting resulted in a reduction in all these parameters.

Figure 17 shows the deviator stress and the K_0^* variation with suction during the wetting and drying processes. At the beginning of the first wetting, the deviator stress q was -27 kPa, implying that K_0^* = 1.125. During the first wetting process the deviator stress increased to 9 kPa, and at this point the K_0^* value reduced to 0.958. Referring to Figure 16, during the first wetting, the specific volume increased by 0.026 and the sample swelled axially by 1.31%. According to the observations made in the test where the overburden pressure was 50 kPa (shallow depth), the sample swelled axially in a significant manner, and it attempted to contract horizontally, but the contraction was accommodated by reducing the horizontal pressure to meet the horizontal strain conditions. However, when the overburden pressure was 200 kPa, the wetting process induced less axial swelling and less increase in specific volume when compared to that observed under an overburden pressure of 50 kPa, but there appears to be a marginal reduction in K_0^* (triggered by a reduction in horizontal pressure) and suggesting that the sample may have also attempted to contract in the lateral direction. The drying process continued until a suction value of 475 kPa, without any violation of horizontal strain conditions at this suction level, and the corresponding K_0^* was approximately 0.35. The subsequent wetting resulted in a recovery of K_0^* and its value at 100 kPa of suction was about 1.0 - a value like that attained during the first wetting phase.

Assessment of the observations

A few of the observations reported above required further discussion or assessment to justify the response of the soils using accepted engineering principles.

Horizontal stress during wetting and drying of KC and BC: At the beginning of the first wetting of KC (shallow depth), the deviator stress q was -65 kPa, implying that the sample was under tension loading as one would expect for the initial K_0^* = 2.30. During the wetting process the deviator stress reduced to -41 kPa, and at this point K_0^* = 1.8. Referring to Figures 14(a) and (b), during this first wetting phase, the specific volume increased by 0.041 (swelling) and the sample swelled axially by 2.0%. However, these observations are contradictory to the changes in the pressure regime, where the deviator stress q increased by about 24 kPa to keep the horizontal strain conditions within the stipulated limits by reducing the horizontal stresses. At odds with this, the increase in specific volume during the first wetting process would imply that the sample wanted to swell in the horizontal (as well as vertical) direction and was restrained to meet the testing conditions (zero horizontal strain) by increasing the horizontal pressure. However, the opposite action, i.e. a reduction in horizontal pressure prevailed during the first wetting, suggesting the initial wetting process may have resulted in contraction of the sample in the horizontal direction and a significant amount of swelling occurring in the axial direction. This observation requires explanation.

The structure of compacted soils plays a crucial role in their behavior, in particular, opposing the pressure-volume response in the vertical and horizontal directions. One of the important factors, often not perceived as an issue is, (a) the lenticular shape of the aggregates with unstable fringes forming the soil mass prepared using static compression Figure 18, and (b) the tendency of the aggregates to swell in the less restrained direction. These attributes could lead to different outcomes than might at first seem logical. The lenticular shape of aggregates with unstable fringes can lead to a localized "preferential swelling" response in the vertical direction. The aggregates would swell overall (in general) upon reduction of suction, however their tendency to swell more in the less restricted direction is often witnessed (Sivakumar *et al.*, 2015; Chen,1987; Carder,1988), and in the present investigation where the vertical pressure was less than the horizontal stress. The authors accept the fact that the above does not rule out less or nil swelling in the horizontal direction upon reduction in suction, but perhaps the horizontal swelling may have been overwhelmed by acute localized collapse triggered by the unstable fringes of the aggregates, thus contributing to a reduction in K_0^* from its initial value upon the first wetting of KC. However, this aspect of an unstable structure leading to potential collapse is an irreversible process and hence, at the start of the drying process, it could be assumed that any potential for collapse of the aggregate structure (lenticular shape with unstable fringes) may have been subdued at the end of the first wetting process and therefore it may not have any relevance during the second wetting process. A question may arise here, as to why this particular response was not witnessed in the case of BC. The aspect of unstable fringes of aggregates giving rise to a potential collapse response upon wetting may also be dependent on clay type. KC is an inert material, However, under certain conditions KC can behave like silt. The reason for this potential confusion may lie in the fact that it has a single plate structure and contains almost uniform particle size. However, BC has a range of particle sizes, and it even has a multi-layered particle structure. In essence, these differences in the physical characteristics could contribute to less unstable fringes on the lenticular shaped aggregates in BC than found in KC.

Swelling response under different overburden pressure: Figure 19 shows a model diagram where the aggregates are packed in a box. Assume the boundaries of the box are semi-flexible (Figure 19a) which will provide some resistance to the aggregates swelling. However, the potential for the aggregate to swell upon wetting will still occur. The aggregates are deformable, and they will therefore swell into the free void or interstitial spaces available between the aggregates and, consequently, there could be a marginal increase in overall volume of the semi-flexible box (Figure 19b). If the boundaries of the box are flexible (Figure 19c), then the swelling nature of aggregates upon wetting could push the boundaries outwards, leading to a situation where the overall volume of the box will increase in a significant manner (Figure 19d). This model is now applied to the present investigations. Wetting under $\overline{\sigma_v}$ = 50 kPa is considered as a "flexible boundary" and that of 200 kPa is considered as a "semi-flexible boundary". Therefore, the aggregates in the sample tested under $\overline{\sigma_v}$ = 200 kPa may find it difficult to expand outwards against high pressure, and therefore swell into macro voids, resulting in less overall swelling. The reverse may hold true in the case of a sample wetted under $\overline{\sigma_v}$ = 50 kPa.

Differences on K_0^* values during wetting and drying:

Figure 20a shows a typical Soil Water Retention Curve (SWRC). An increase in suction will deplete water from the voids and the soil will undergo desaturation when the suction exceeds the air entry value of the soil. Suppose the soil is subsequently taken through wetting and reducing suction. The wetting process will follow a different path. If the process is repeated several times, there will be a series of scanning curves, reflecting the state of the soil and dependent on whether it was on a drying path or wetting path. The important observation from the above is that, at a given value of suction, the soil may have a higher degree of saturation during the drying process than during the wetting process. This is largely due to different mechanisms prevailing during the emptying and filling processes. Consider two cases on a SWRC at similar suction values; suppose the soil is on the drying path on the SWRC, then it would have a higher number of water menisci forming at the aggregate contacts, giving rise to stability of the soil. The reverse may hold true if the soil were to be on a wetting path on the SWRC. It can therefore be conjectured that soil may be stiffer if it were to be on the course of a drying process as opposed to a wetting process at a given suction. It could therefore lead to a situation where K_0^* during the wetting process was higher than during the drying process at a given suction as illustrated in Figure 20b. This is what is observed in the present research upon repeated wetting and drying processes, abating the fact that the first wetting inflicted some irrecoverable responses in terms of K_0^* in KC due to its unstable structure.

CONCLUSIONS

The consequence of climate change on planet Earth is clearly apparent and one of the direct pieces of evidence is the prolonged dry summers and wet winters that we now endure. These unprecedented events are straining our vital infrastructure which is both interacting with and impacting our soils. The topic examined in this thesis refers to the performance of a retaining wall backfilled with soils. Investigations were carried out on samples of KC and BC subjected to wetting and drying cycles. These processes were conducted while the samples were restrained from horizontal contraction or expansion.

- The earth pressure coefficient K_0^* of compacted clay is generally assumed to have a value of unity in compacted clays. However, the work carried out to replicate the field compaction process has clearly shown that the K_0^*values can be very high for both clays at shallow depths.

- It was anticipated that the wetting process could instigate an increase in K_0^* value. However, some interesting observations were made in the case of Kaolin Clay. Unlike BC, the first wetting of KC resulted in a reduction in K_0^*, value. The reason for this was attributed to the unstable nature of fringes on the lenticular shaped aggregates.
- Repeated wetting after drying resulted in no significant increase in K_0^* values (compared to the initial value) apart from a reduction in Kaolin Clay upon first wetting.
- Drying resulted in the formation of tension cracks. The suction at which they began to form increased with overburden pressure.
- Wetting and drying resulted in a case where the value of K_0^* was high during wetting than during drying, at a given suction. These observations are supported with the concept often adopted for SWRC.

ACKNOWLEDGEMENT

The funding for the research was provided by Engineering and Physical Science Research Council (EPSRC) Grant No. (Project code. R1828NBE, EPSRC Reference: EP/R005834/1)

AVAILABILITY OF DATA

Some or all data, models, or code that support the findings of this study are available from the corresponding author upon reasonable request.

REFERENCES

Alonso, E. E, Gens, A, and Josa, A. (1990). A constitutive model for partially saturated soils. *Géotechnique*, **Vol 40(3)**, pp 405-430.

ASTM D1557-12 (Modified Proctor-ASTM D1557/AASHTO T180). (2021). Standard Test Methods for Laboratory Compaction Characteristics of Soil Using Modified Effort (56,000 ft-lbf/ft^3 (2,700 kN-m/m^3)). *American Society for Testing and Materials Standards*.

BS1377-4:1990. Methods of test for soils for civil engineering purposes, Part 4: Compaction-related tests. *British Standard Institution*.

Carder, D. R. (1988). Earth pressures on retaining walls and abutments. *Ground Engineering*, **Vol 21(5)**, pp 7–10.

Chen, F. H. (1987). Lateral expansion pressure on basement walls. *Proceedings of the 6th international conference on expansive soils*, New Delhi, India vol 1, pp 55–59. Boca Raton, FL, USA: CRC Press.

Clayton, C.R.I., Symons, I.F., Hiedra, J.C., (1991). The pressure of clay backfill against retaining structures. *Canadian Geotechnical Journal*, **Vol 28(2)**, pp 282-297.

COP27 (2023). Official sustainability report. Government of the Arab Republic of Egypt Official Host Country 2022 United Nations Climate Change Conference, Sharm El-Sheikh, 6th – 18th November 2022.

Cui, Y. J, and Delage, P. (1996). Yielding and plastic behaviour of an unsaturated compacted silt. *Géotechnique*, **Vol 46(2)**, pp 291-311.

Doran, I. G. (1992). The subsoils of Northern Ireland. *The Structural engineer (Geology),* **Vol 70(7)**, pp 135-138.

Duncan, j.M., Williamns, G.W., Sehn, A.L., and Seed, R.B>, (1991). Estimating earth pressure due to compaction. Jurnal of geotechnical Engineering, Vol 117, No 12, pp 1833-1842

Filts, D.M and Duncan, J.M., (1996). Earth pressures due to compaction: comparison of theory with laboratory and field behavior. Journal of Transport Res Board, No.1526, pp 28-37

Fredlund, D. G., Morgenstern, N. R., and Widger, R.A. (1978). The shear strength of unsaturated soils. *Canadian Geotechnical Journal,* **Vol 15(3)**, pp 313-321

Giles, D.P. and Griffiths, J.S. (2020). Geological Hazards in the UK: Their Occurrence, Monitoring and Mitigation – Engineering Group Working Party Report. Geological Society, London, Engineering Geology Special Publications 2020 DOI: 10.1G144/egsp29.

Han, Z., Zhang, P., Zou, W, Fan, K., Vanapalli, S. and Wan, L., (2024). At-rest lateral earth pressure of compacted expansive soils: Experimental observations and predictive approach. Journal of Rock Mechanics and Geotechnical Engineering, Vol 16, pp 1425-1435

Highways Agency, Scottish Development Department, The Welsh Office and The Department for the Environment for Northern Ireland (1995). *Earthworks design and preparation of contract documents, HA 44/91; Design manual for roads and bridges, Geotechnical drainage*, **Vol. 4**. London, UK: Her Majesty's Stationery Office.

Highways Agency, Scottish Development Department, The Welsh Office and The Department for the Environment for Northern Ireland (2004). *Manual of contract documents for highways works MCHW1; Specification for highways works*, Series 600. London, UK: Her Majesty's Stationery Office.

Hilf, J. N., (1956). An investigation of pore water pressure in compacted cohesive soils. Technical memorandum 654. U.S. Department of Interior Bureau of Reclamation, Denver. https://doi.org/10.1139/t91-034.

Ingold, T.S., 1979. Effects of compaction on retaining walls, Geotechnique, Vol 29, No. 3 pp 265-283

Jeyaraj, T. (2023). Stress regime in compacted fills during wetting and drying cycles under laterally restrained conditions. PhD thesis, Queen's University Belfast.

Lloret, A., Villar, M. V., Sanchez, M., Gens, A., Pimtado, X., Alonso, E. E. (2003). Mechanical behaviour of heavily compacted bentonite under high suction changes. *Géotechnique* **Vol.53(1)**, pp27–40.

Loveridge, F., Spink, T., O'Brien, T., Briggs, K., & Butcher, D. (2010). The impact of climate and climate change on infrastructure slopes with particular reference to southern England. *Quarterly Journal of*

Engineering Geology and Hydrogeology, **Vol 43(4)**, 461-472. https://doi.org/10.1144/1470-9236/09-050.

Lu, N., Likos, W. J. (2004). Unsaturated soil mechanics. New York, NY, USA: Wiley.

Lynch, K., Sivakumar, V., Tripathy, S., & Hughes, D. (2019). Development of a laboratory technique for obtaining soil water retention curves under external loading in conjunction with high-capacity tensiometers. *Géotechnique*, **Vol 69(4)**, 320–328. https://doi.org/10.1680/jgeot.17.p.176.

Mawditt, J. M. (1989). Discussion: Conventional retaining walls: pilot and full-scale studies. *Proc. Instn Civ. Engrs*, *Part 1*, **Vol 86, (5)**, pp 980–986.

Murray, T. and Sivakumar, V. , (2010). Unsaturtaed soils (fundamental apparoch to interpretation of soil behaviour) . Blackwell publishers, UK

NOAA (2024). National Centers for Environmental Information, Monthly Global Climate Report for November 2024. Published online December 2024, https://www.ncei.noaa.gov/access/monitoring/monthly-report/global/202411.

Proctor, R. R. (1933). Fundamental Principles of Soil Compaction. *Engineering News-Record*, **Vol 111(9, 10, 12, and 13)**.

Rising, J., Dietz, S., Dumas, M., Khurana, R., Kikstra, J., Lenton, T., Linsenmeier, M., Smith, C., Taylor, C., Ward, B. (2022). What will climate change cost the UK? Risks, impacts and mitigation for the net-zero transition. London: Grantham Research Institute on Climate Change and the Environment, London School of Economics and Political Science.

Simons, I.F. and Clayton, C.R.I (1992). Earth pressure on backfilled retaining walls. Ground Engineering

Sivakumar, V., Donohue, S., Rødvand, L., Nanda, S. and Tripathy, S. (2018). Behaviour of normally consolidated claycontaining isolated solid inclusions. Proceedings of the Institution of Civil Engineers – Geotechnical Engineering 171(4): 345–35.

Sivakumar, V., Navaneethan, T., Hughes, D. and Gallagher, G. (2009).“An assessment of the earth pressure coefficient in overconsolidated clays.” ***Géotechnique*,** Vol. 59(10), pp. 825-838.

Sivakumar, V., Navaneethan, T., Hughes, D. and Gallagher, G., 2009. 825An assessment of the earth pressure coefficient in overconsolidated clays. Geotechnique, 59, No. 10, 825–838 [doi: 10.1680/geot.8.P.033]825.

Sivakumar, V., Sivakumar, R., Murray, E.J., Mackinnon, P. and Boyd, J. (2010a). Mechanical Behaviour of Unsaturated Kaolin: (with Isotropic and Anisotropic Stress History) Part 1: Wetting and Compression Behaviour. *Géotechnique*, **Vol 60(8)**, pp 581-594.

Sivakumar, V., Zaini, J. and Gallapoli, D. (2015**).** Wetting of compacted clays under laterally restrained conditions: Initial state, overburden pressure and mineralogy**.” Geotechnique,** Vol. 65, No. 1.

Sivakumar, V., Zaini, J., Gallipoli, D., and Solan, B. (2015). Wetting of compacted clays under laterally restrained conditions: Initial state, overburden pressure and mineralogy. *Géotechnique*, **Vol 65(2)**, pp 111–125. https://doi.org/10.1680/geot.14.P.019.

Skempton, A. W. (1964). Long term stability of clay slopes. *Géotechnique*, **Vol 14(2)**, pp 77–101.

Toll, D.G. 1999. "A Data Acquisition and Control System for Geotechnical Testing", in B. Kumar, B.H.V. Topping, (Editors), "Computing Developments in Civil and Structural Engineering", Civil-Comp Press, Edinburgh, UK, pp 237-242, 1999. doi:10.4203/ccp.63.7.3

Toll, D.G., Abedin, Z., Buma, J., Cui, Y., Osman, A., and Phoon, K. (2012). The impact of changes in the water table and soil moisture on structural stability of buildings and foundation systems: Systematic review CEE10-005 (SR90). *Natural Environment Research Council under the Living with Environmental Change Programme.* pp 21-22.

Wheeler, S. J, and Sivakumar, V. (1995). An elasto-plastic critical state framework for unsaturated soil. *Géotechnique*, **Vol 45(1)**, pp 35-53.

Table 1 Basic characteristics

Soil Type	Liquid Limit %	Plastic Limit %	Maximum dry density kg/m^3	Optimum water content %
Kaolin Clay	70	31	1458	28.0
Belfast Clay	56	27	1640	22.7

Table 2 Initial stress conditions after compression

Soil type	Depth (m)	Net Vertical stress (kPa)	Net Horizontal stress (kPa)	Suction (kPa)
Kaolin Clay	2.5	50	115	525
	10.0	200	225	475
Belfast Clay	2.5	50	150	405
	10.0	200	250	350

Table 3 Suction changes during wetting and drying

Soil type	Depth (m)	1st wetting (kPa)	1st drying(kPa)	2nd wetting (kPa)
Kaolin Clay	10.0	475-375-275-175-100	100-175-275-375-475	475-375-275-175-100-20
	2.5	525-475-425-325-225-100	100-200-300-400	400-300-200-100-20
Belfast Clay	2.5	400-300-200-100	100-200-300-400-500	500-400-300-200-100
	10.0	350-250-150-100	100-200-300-400-500-600	600-500-400-300-200-100

List of Figures

Figure 9 Initial stress conditions

Figure 10 Volumetric response during drying process at the 2.5 m depth (BC)

(a) Specific volume

(b) Axial strain

(c) Degree of saturation

Figure 11: Pressure evolution during wetting and drying 2.5 m depth (BC)

(a) Deviator stress

(b) Earth pressure coefficient K_o^*

Figure 12: Volumetric response during drying process at the 10.0 m depth (BC)

(a) Specific volume

(b) Axial strain

(c) Degree of saturation

Figure 13: Pressure evolution during wetting and drying 10.0 m depth (BC)

(a) Deviator stress

(b) Earth pressure coefficient K_o^*

Figure 14: Volumetric response during drying process at the 2.5 m depth (KC)

(a) Specific volume

(b) Axial strain

(c) Degree of saturation

Figure 15 : Pressure evolution during wetting and drying 2.5m depth (KC)

(a) Deviator stress

(b) Earth pressure coefficient K_o^*

Figure 16: Volumetric response during drying process at the 10.0m depth (KC)

(a) Specific volume

(b) Axial strain

(c) Degree of saturation

Figure 17 : Pressure evolution during wetting and drying 10.0m depth (KC)

(a) Deviator stress

(b) Earth pressure coefficient K_o^*

Figure 18:The aggregates deform into a lenticular shape

(a) Semi-Flexible boundary (initial)

(b) Semi-Flexible boundary (after saturation)

(c) Flexible boundary (initial)

(d) Flexible boundary (after saturation)

Figure 19: A model diagram for illustrating swelling process

Figure 20 SWRC and K_0^* variations during wetting and drying

(a) A typical SWRC for soils

(b) K_o^*variations during wetting and drying

Thanking you for accepting, our article. As suggested, we have now revised the figures 6c and 7c in which the X axis provides direct values of pressure.
Sivakumar-V

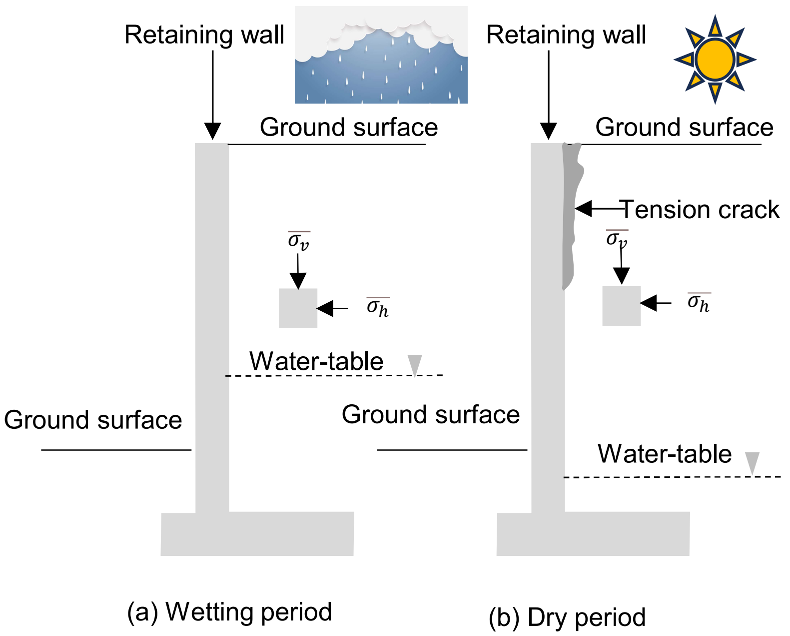

Figure 1: Compacted/natural clay behind a retaining structure

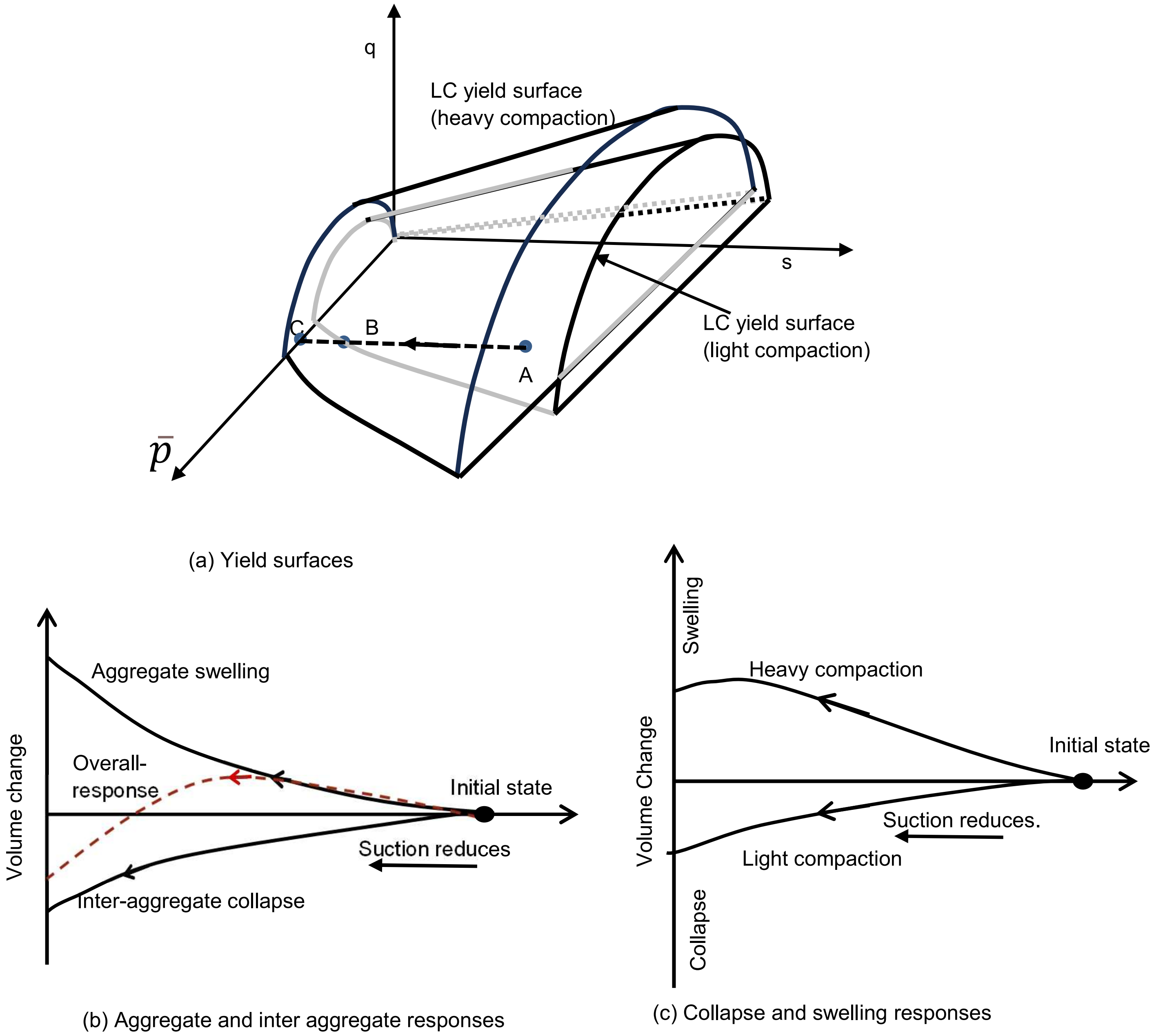

Figure 2 Constitutive modelling of unsaturated soils

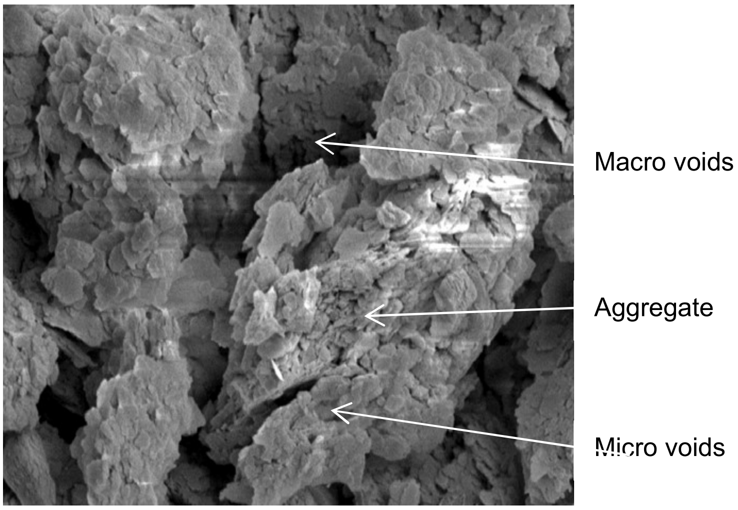

Figure 3 Bi-modal pore structure of compacted soils

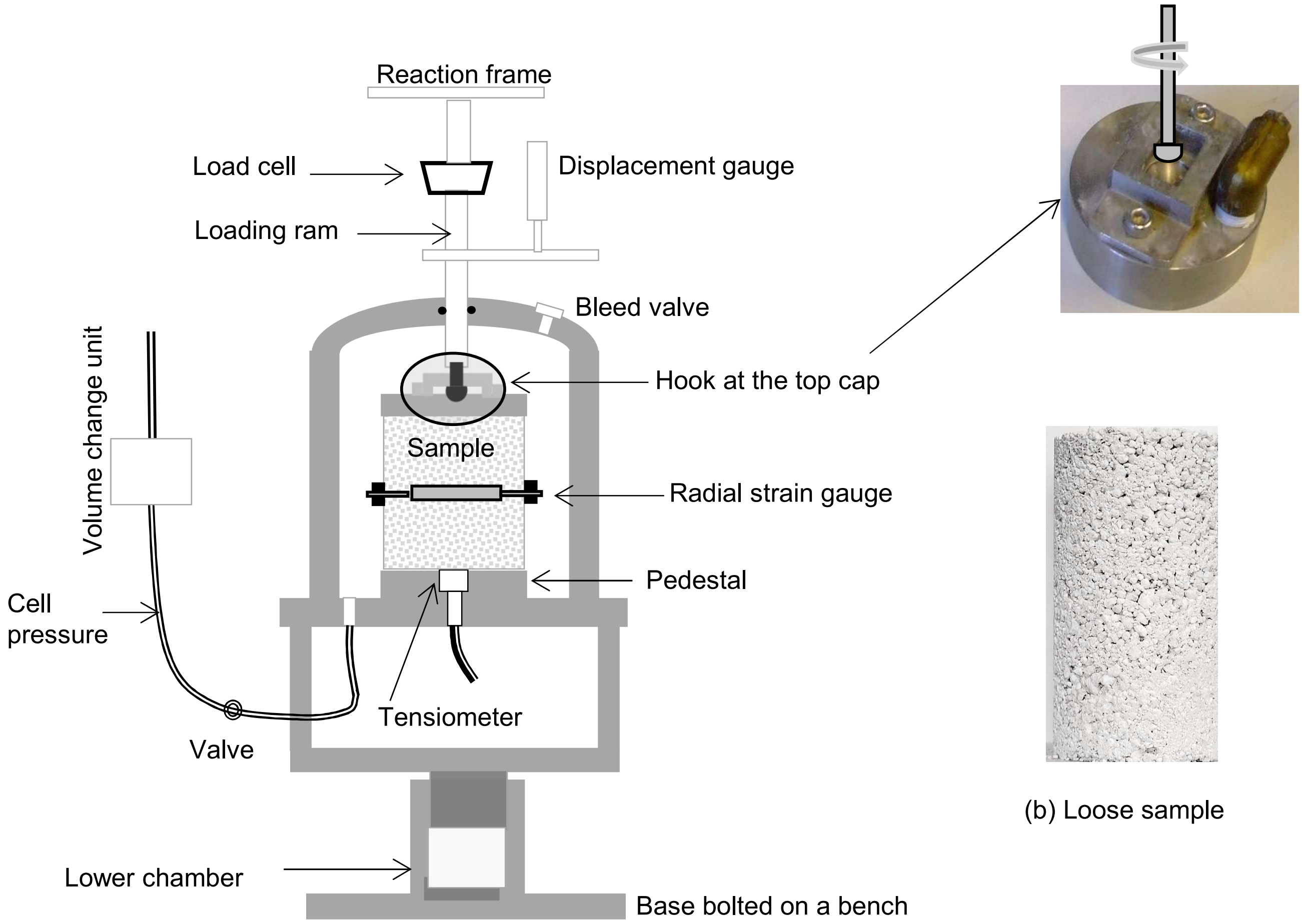

(a) Stress path cell

(b) Loose sample

Figure 4: Testing chamber

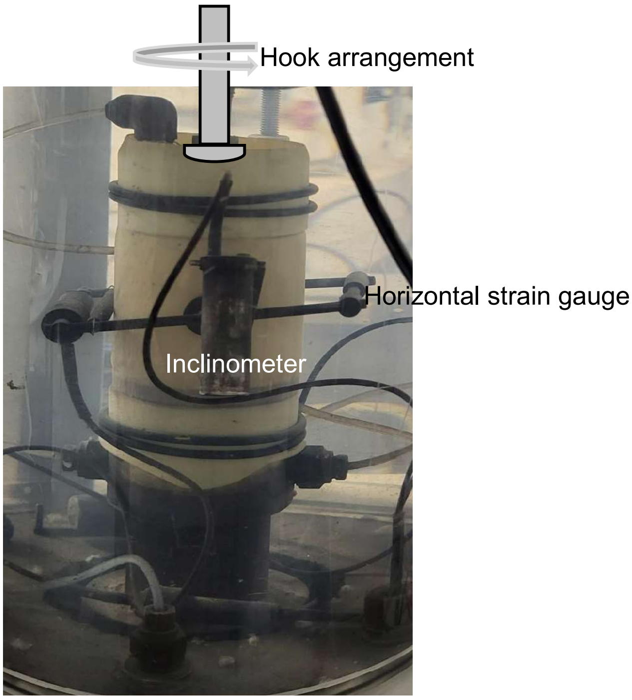

Figure 5: Testing arrangement for wetting and drying process

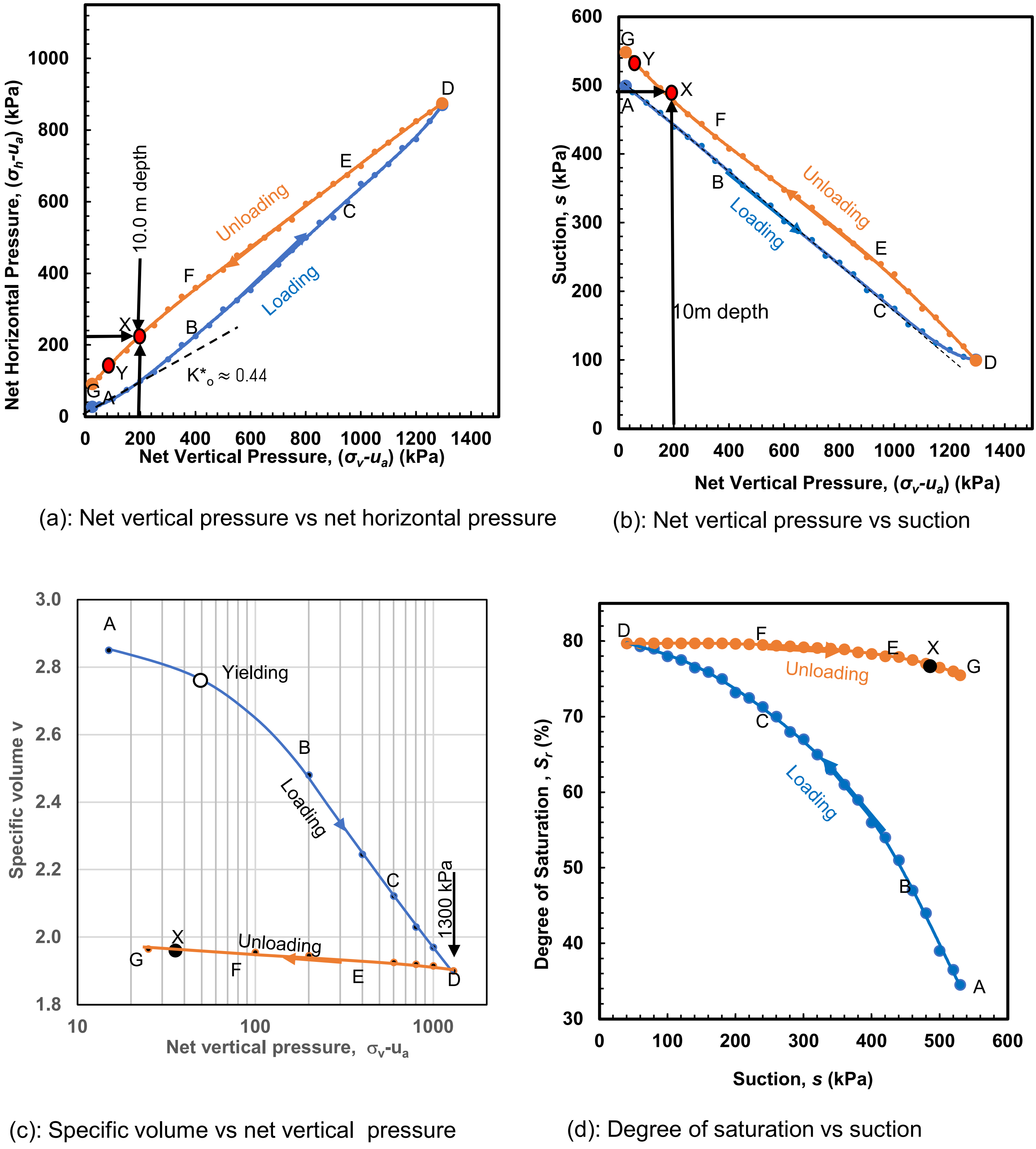

Figure 6: Evolutions of pressure and strain variables (KC)

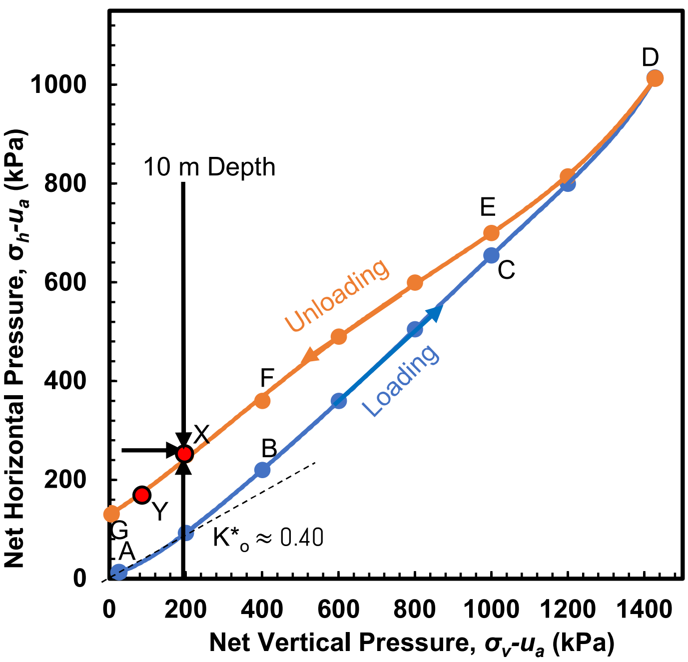

(a): Net vertical pressure vs net horizontal pressure

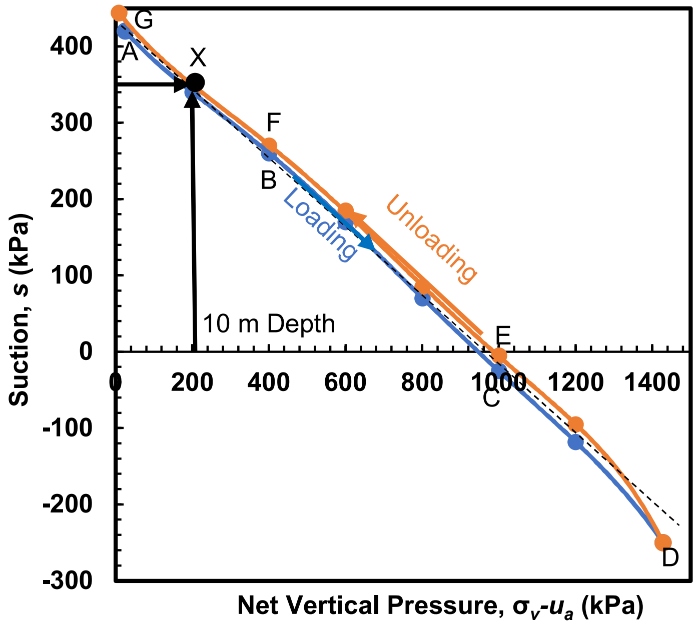

(b): Net vertical pressure vs suction

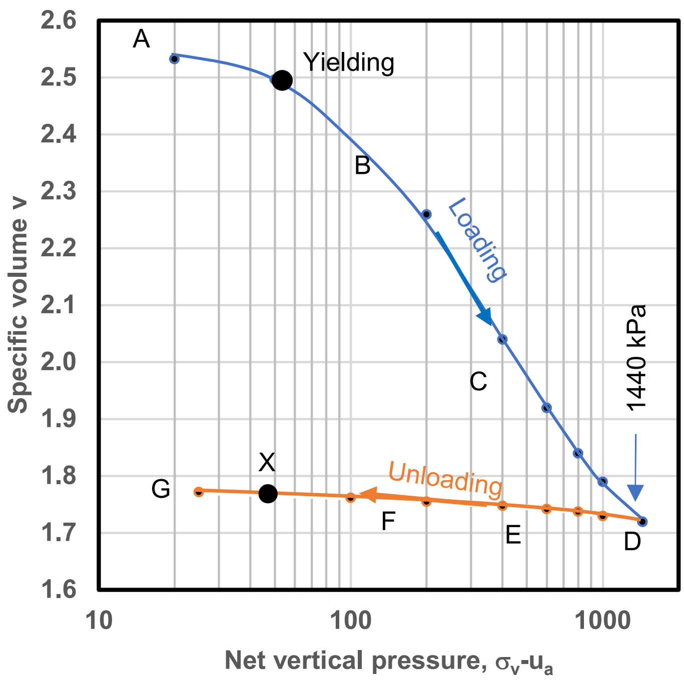

(c): Specific volume vs net vertical pressure

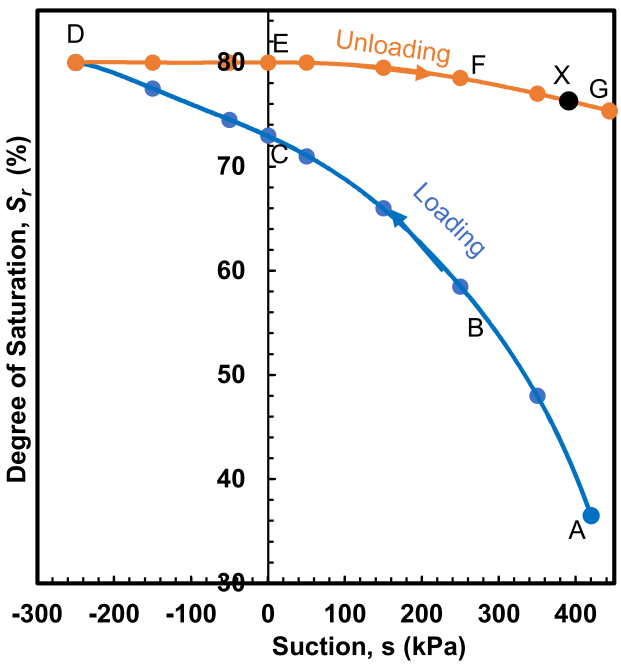

(d): Degree of saturation vs suction

Figure 7 Evolutions of pressure and strain variables (Belfast Clay)

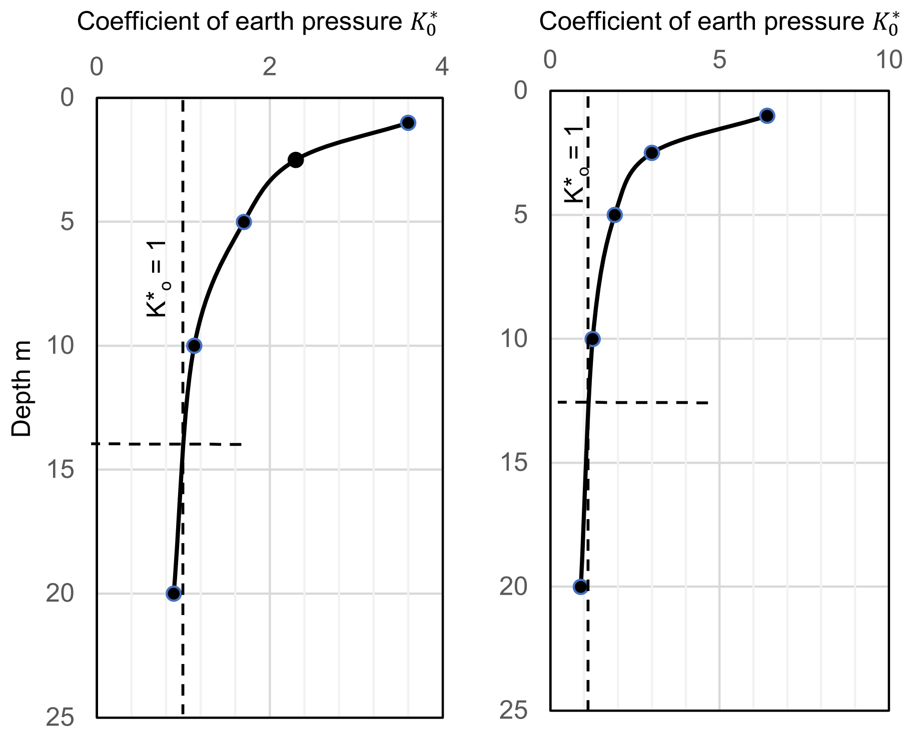

(a) KC

(a) BC

Figure 8:The profiles of $K_0^*$with depth for three different soils

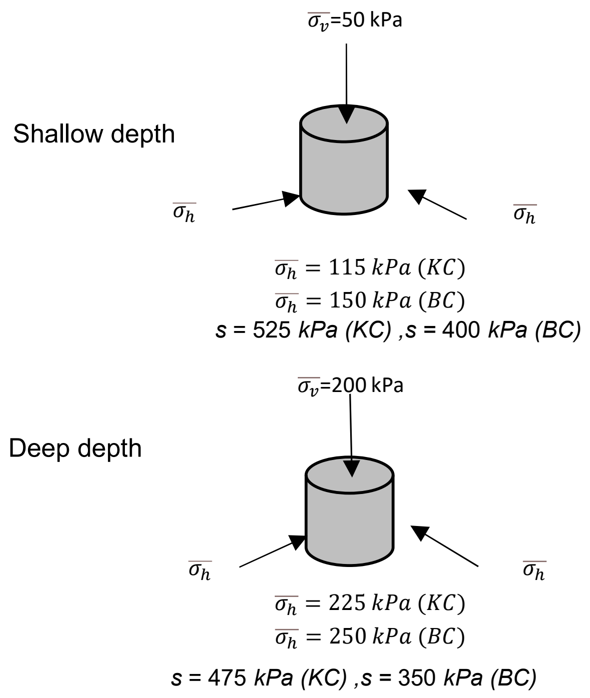

Figure 9 Initial stress conditions

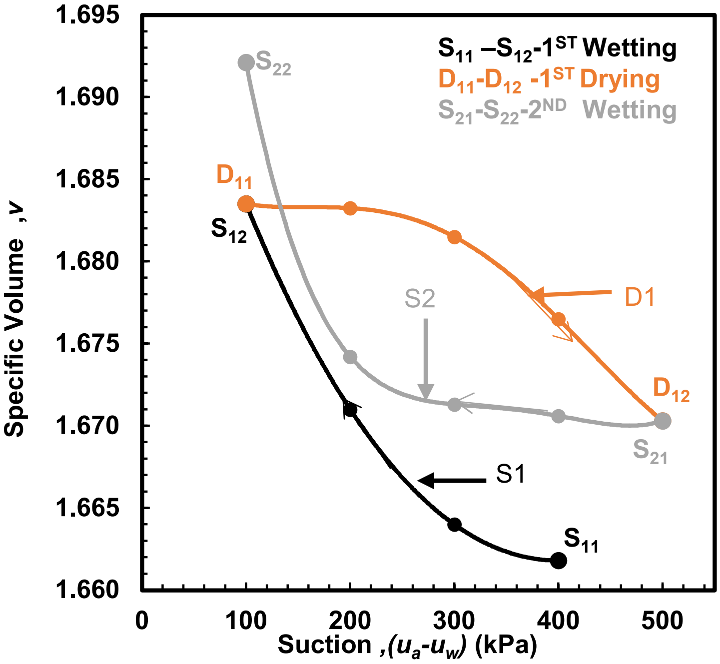

(a): Specific volume

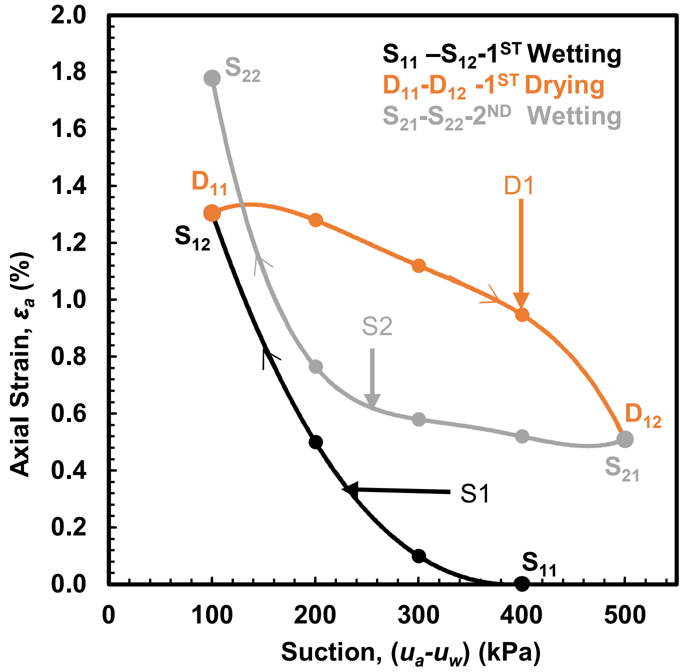

(b) Axial strain

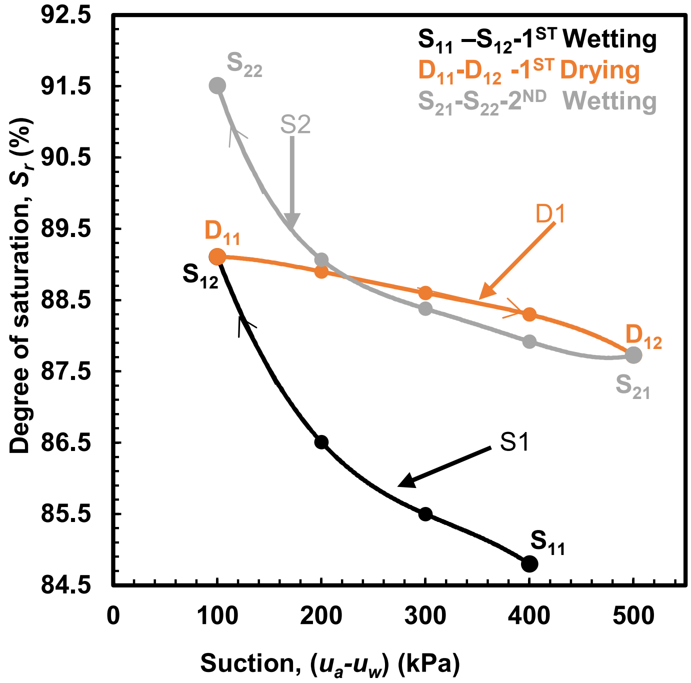

(c): Degree of saturation

Figure 10 Volumetric response during drying process at the 2.5 m depth (BC)

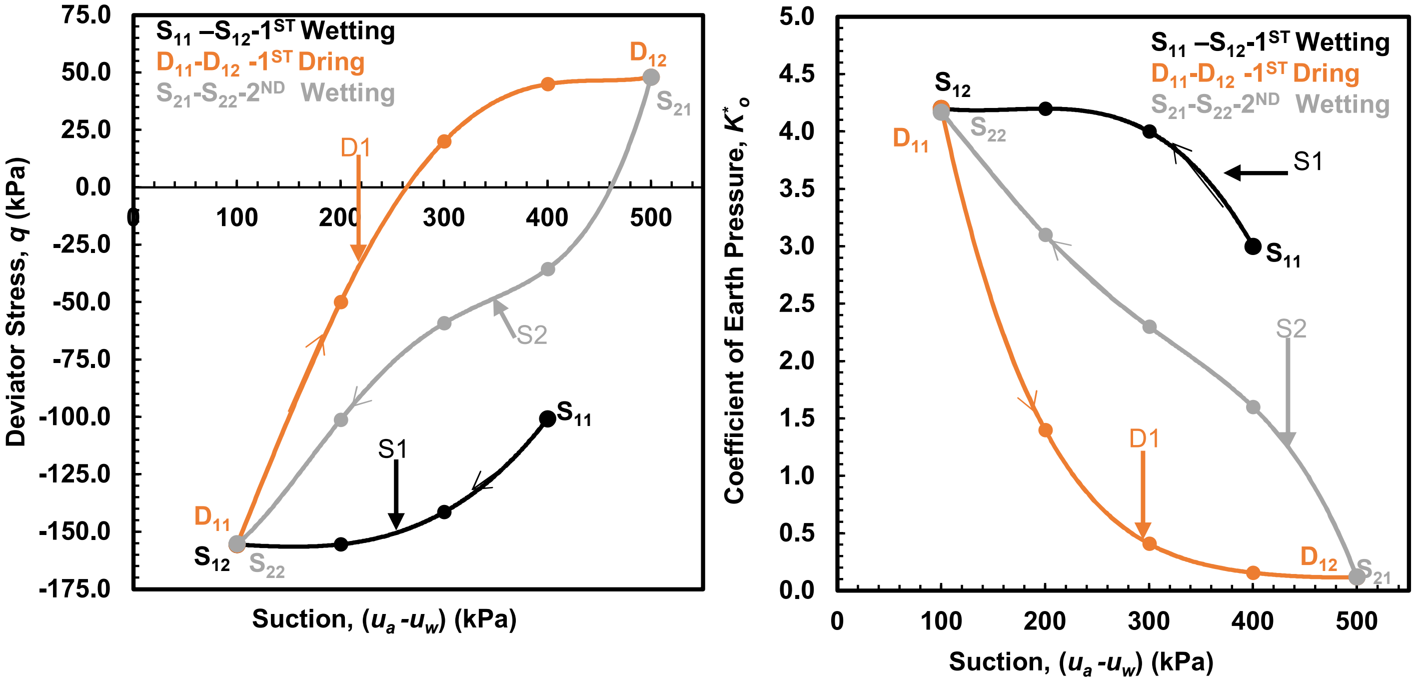

(a): Deviator stress (b) Earth pressure coefficient K^*_0

Figure 11: Pressure evolution during wetting and drying 2.5 m depth (BC)

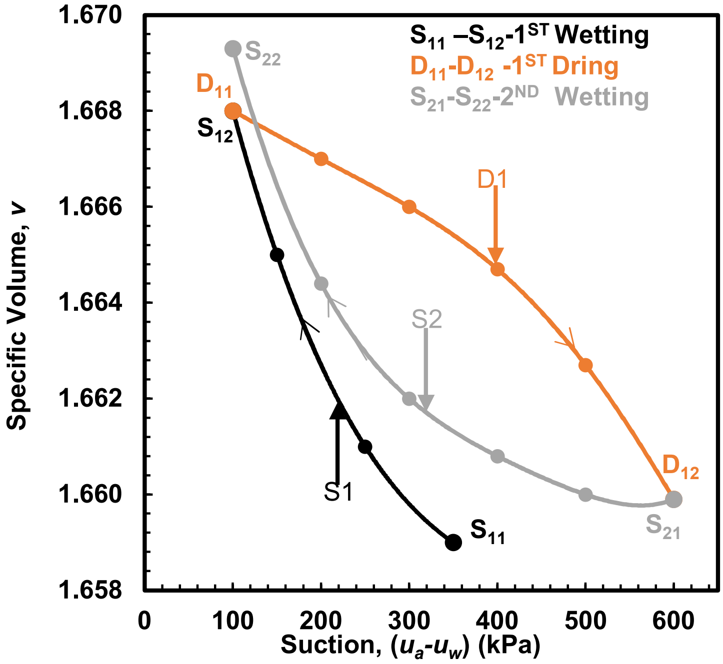

(a): Specific volume

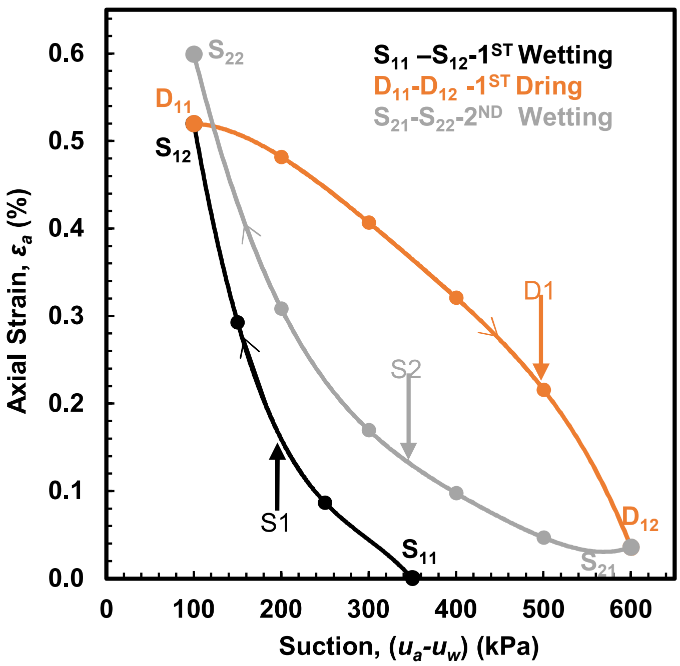

(b) Axial strain

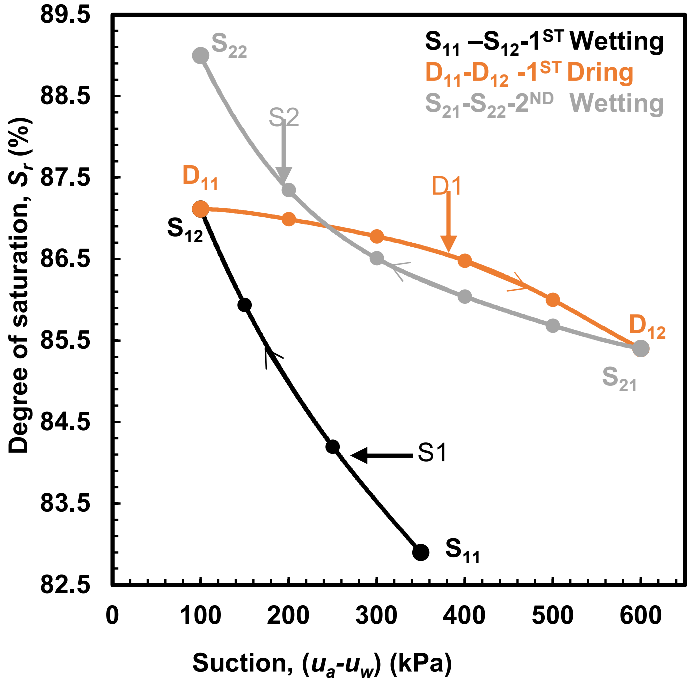

(c): Degree of saturation

Figure 12: Volumetric response during drying process at the 10.0 m depth (BC)

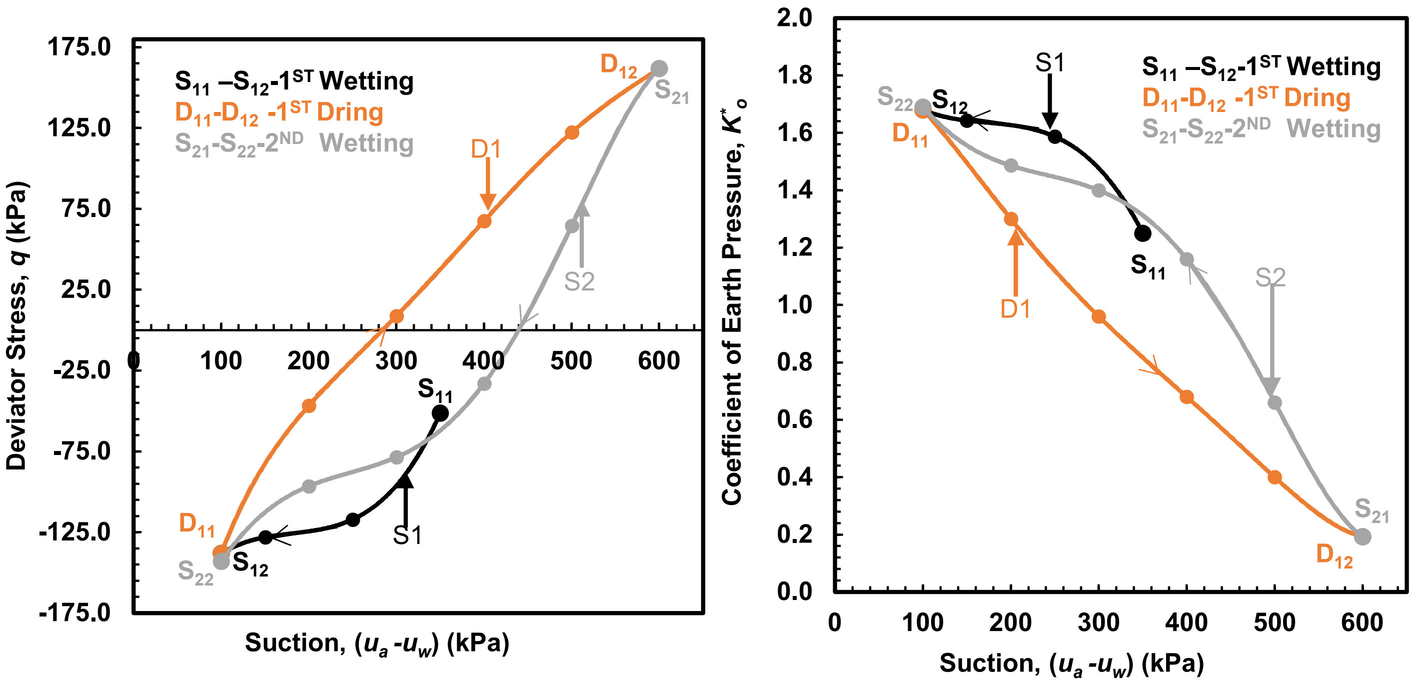

(a): Deviator stress

(b) Earth pressure coefficient K^{*}_{0}

Figure 13: Pressure evolution during wetting and drying 10.0 m depth (BC)

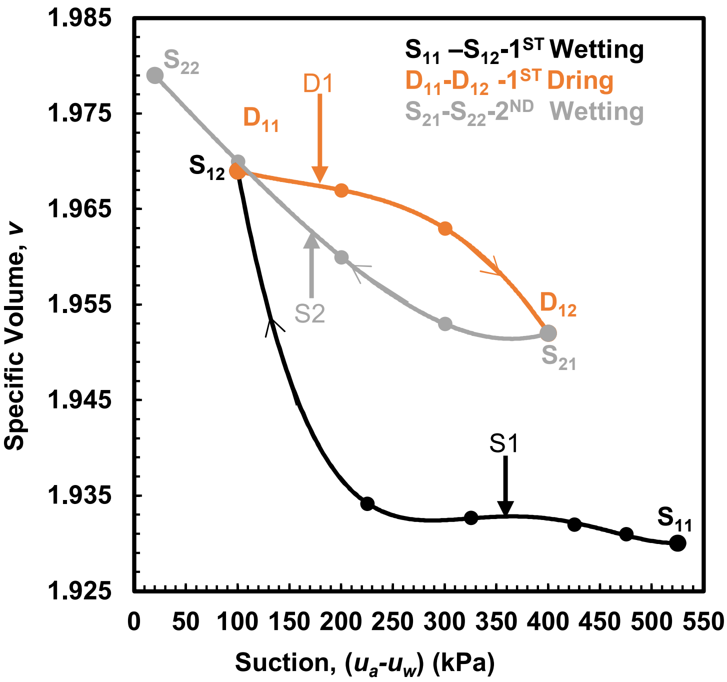

(a): Specific volume

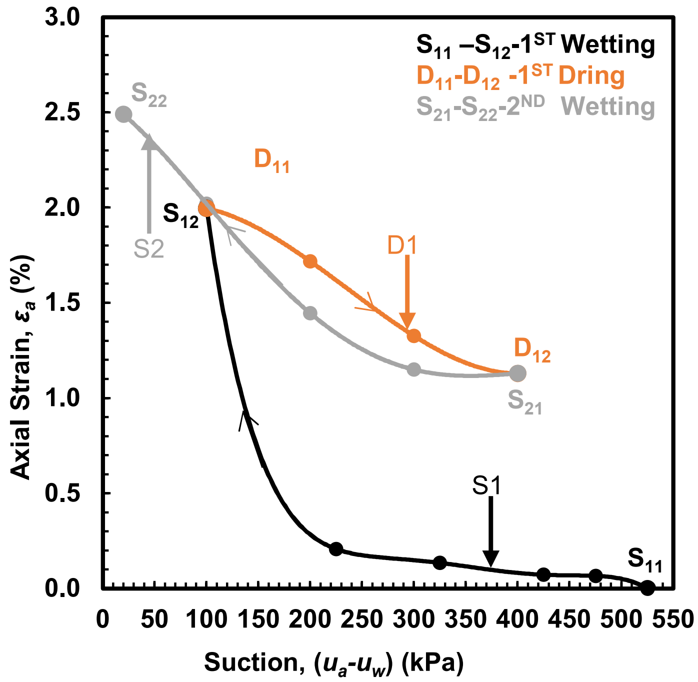

(b) Axial strain

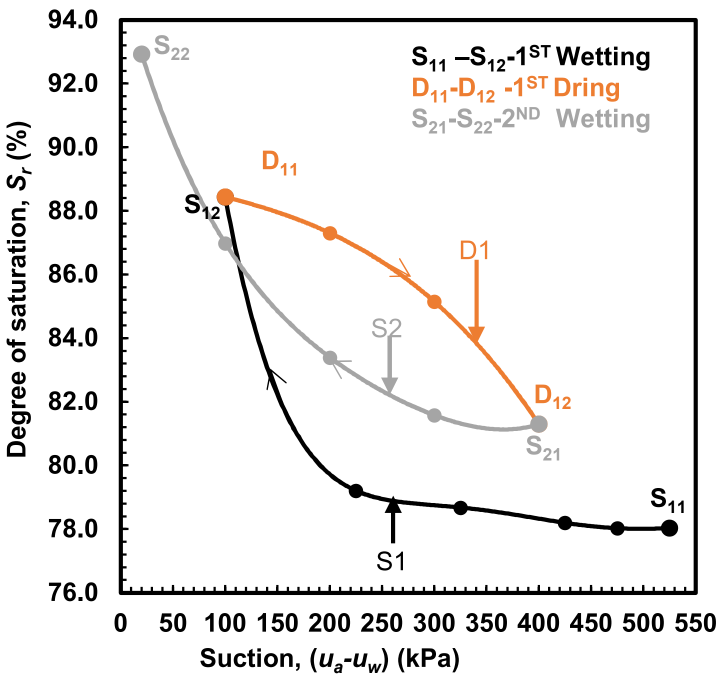

(c): Degree of Saturation

Figure 14: Volumetric response during drying process at the 2.5 m depth (KC)

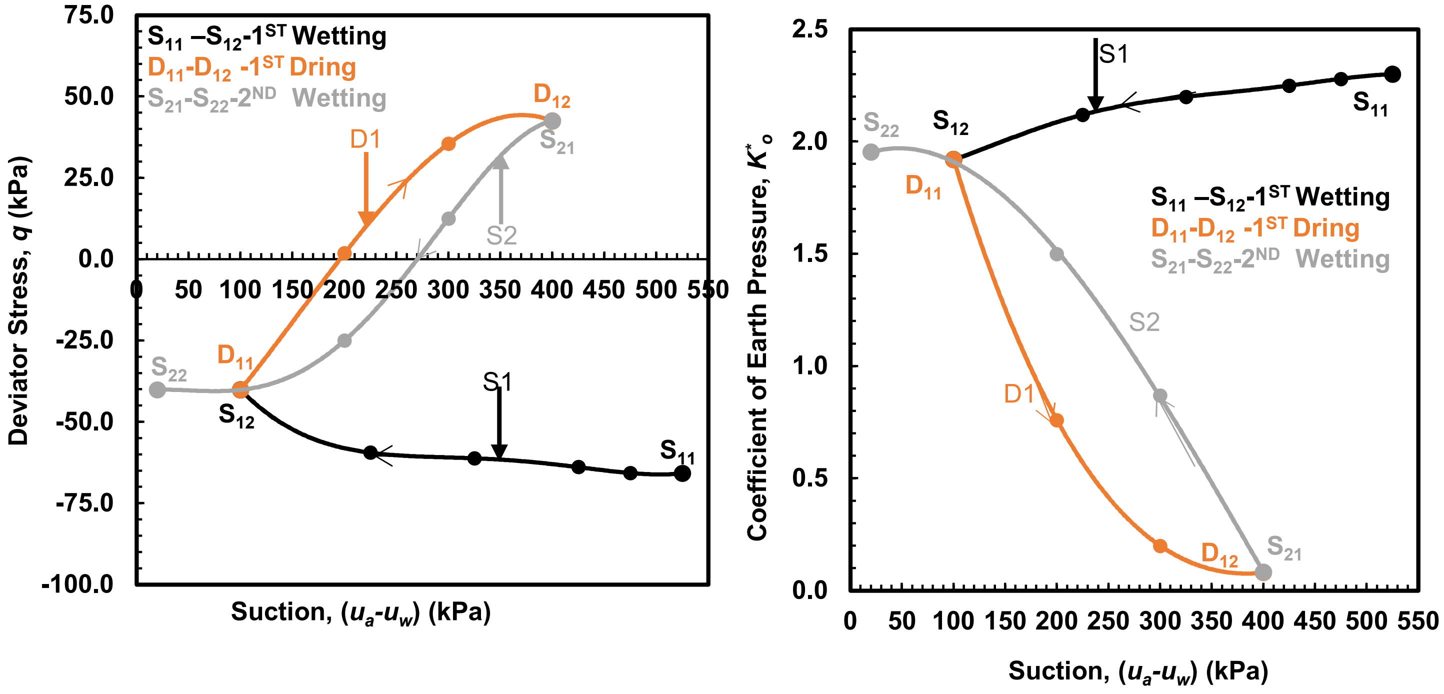

(a): Deviator stress

(b) Earth pressure coefficient K^{*}_{0}

Figure 15 : Pressure evolution during wetting and drying 2.5m depth (KC)

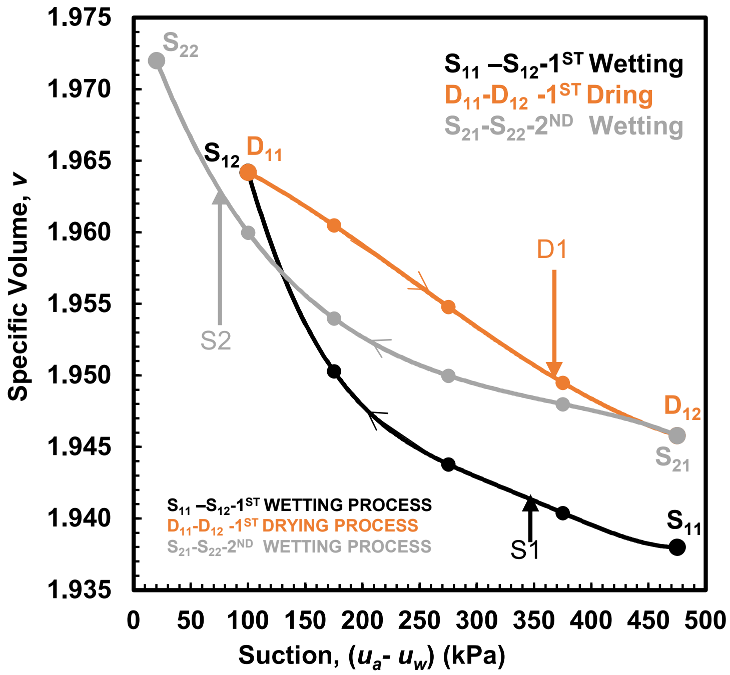

(a): Specific volume

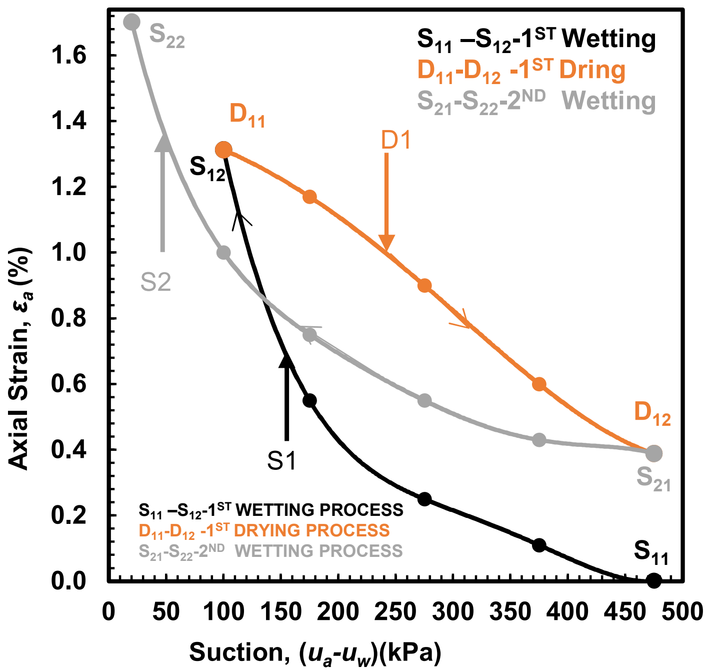

(b) Axial strain

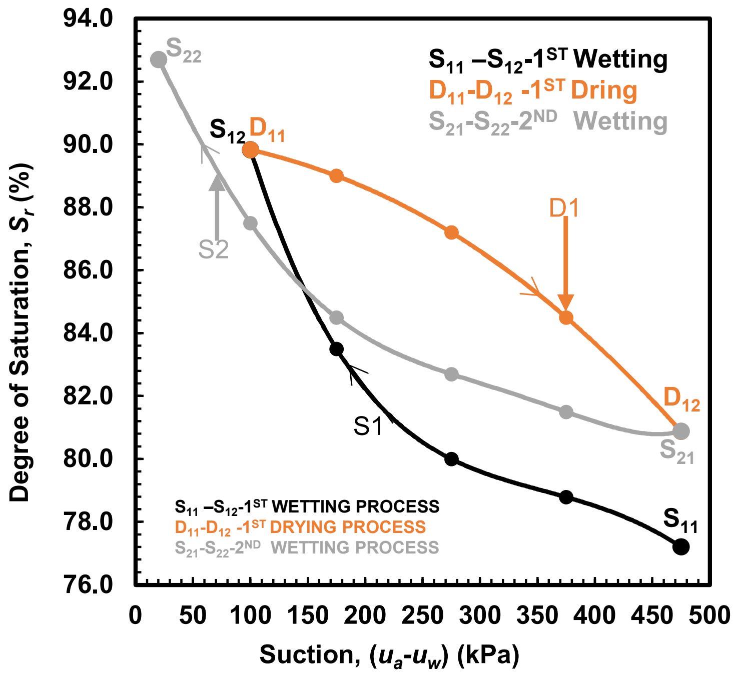

(c): Degree of saturation

Figure 16: Volumetric response during drying process at the 10.0m depth (KC)

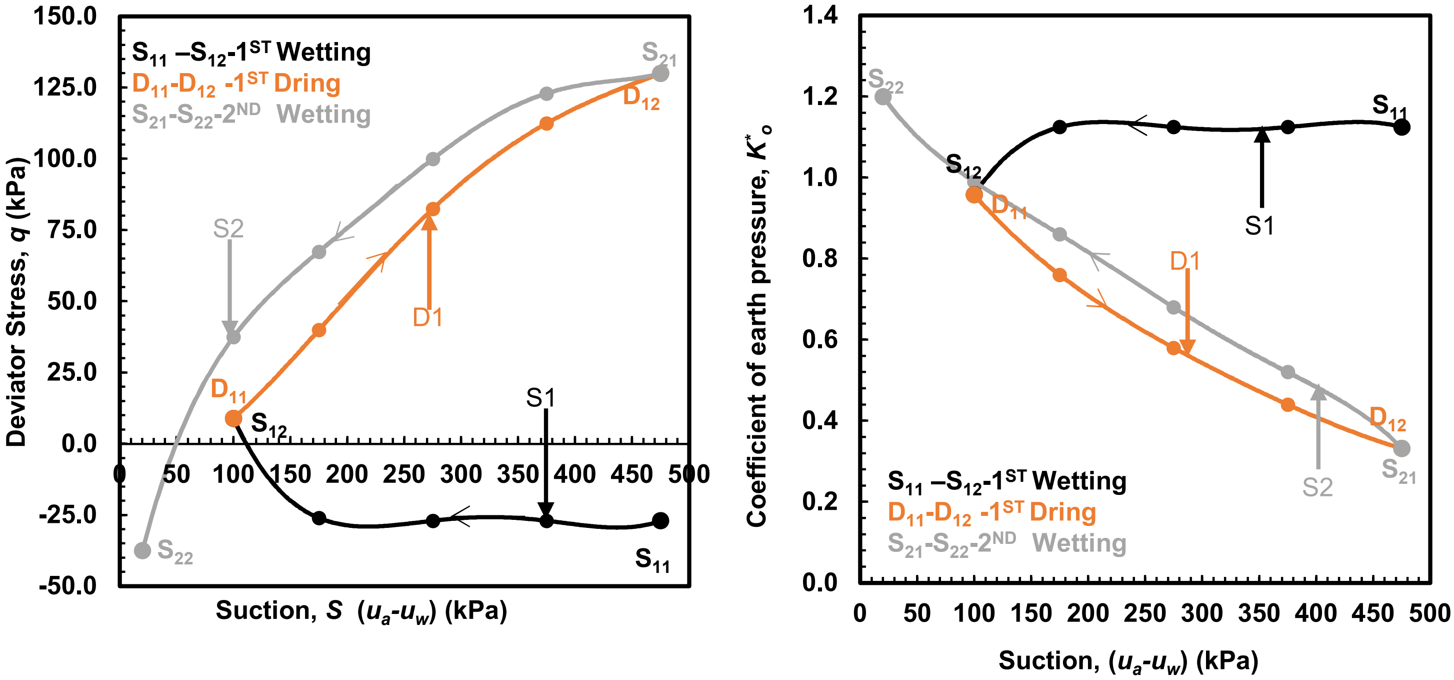

(a): Deviator stress

(b) Earth pressure coefficient K^{*}_{0}

Figure 17 : Pressure evolution during wetting and drying 10.0m depth (KC)

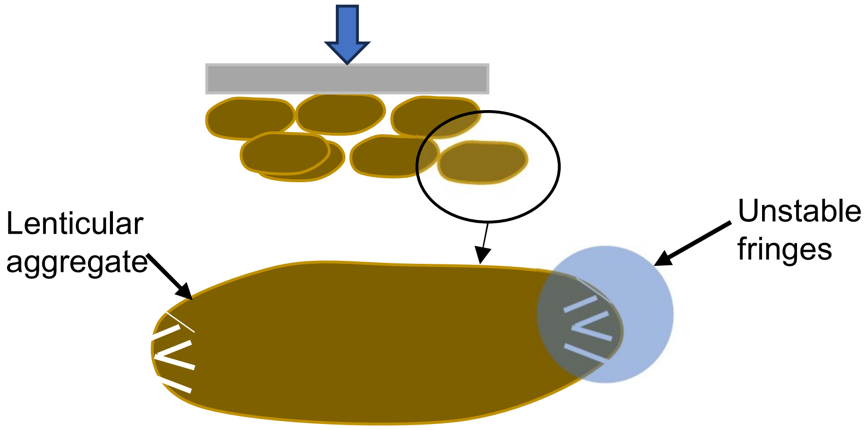

Figure 18:The aggregates deform into a lenticular shape

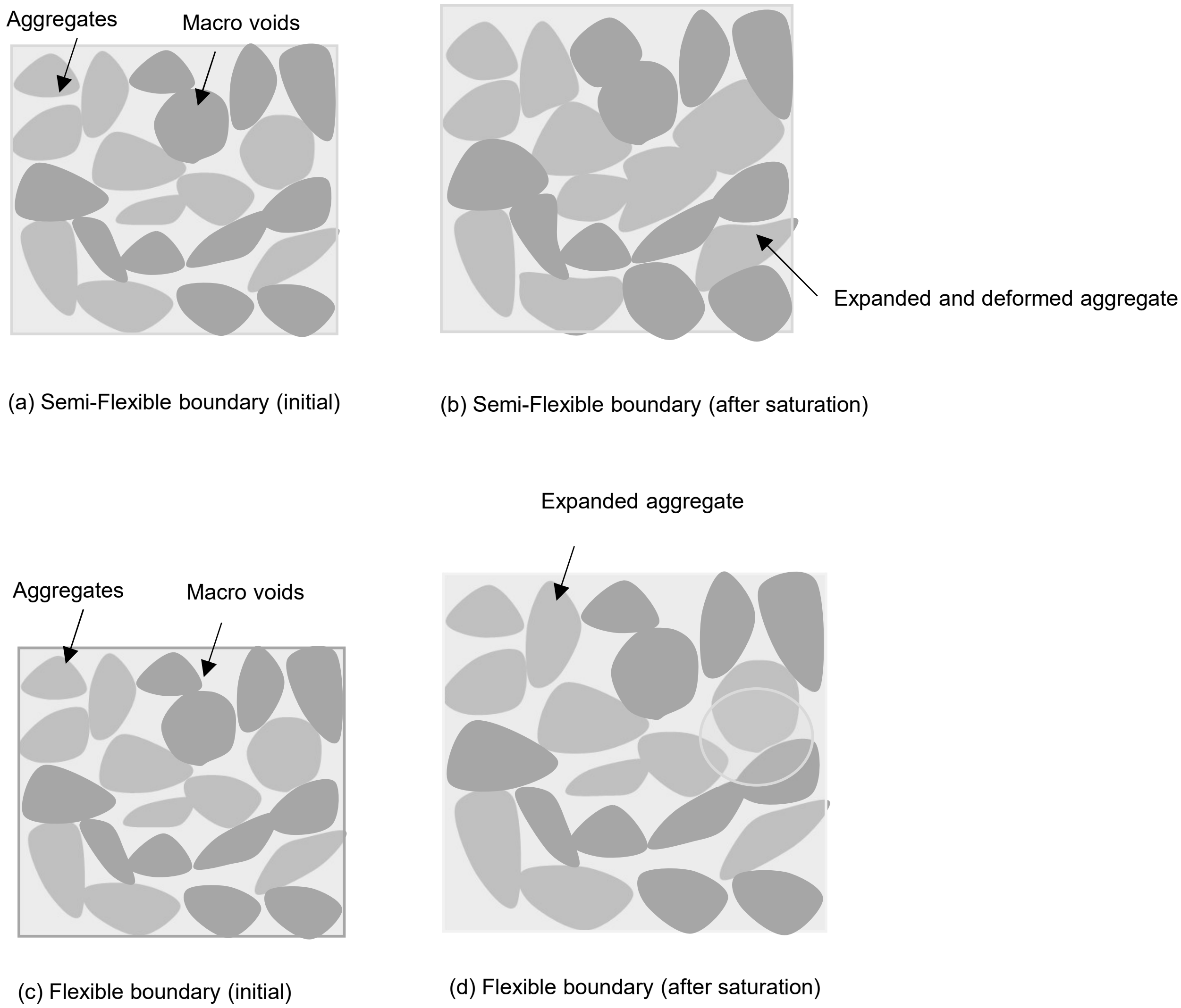

Figure 19: A model diagram for illustrating swelling process

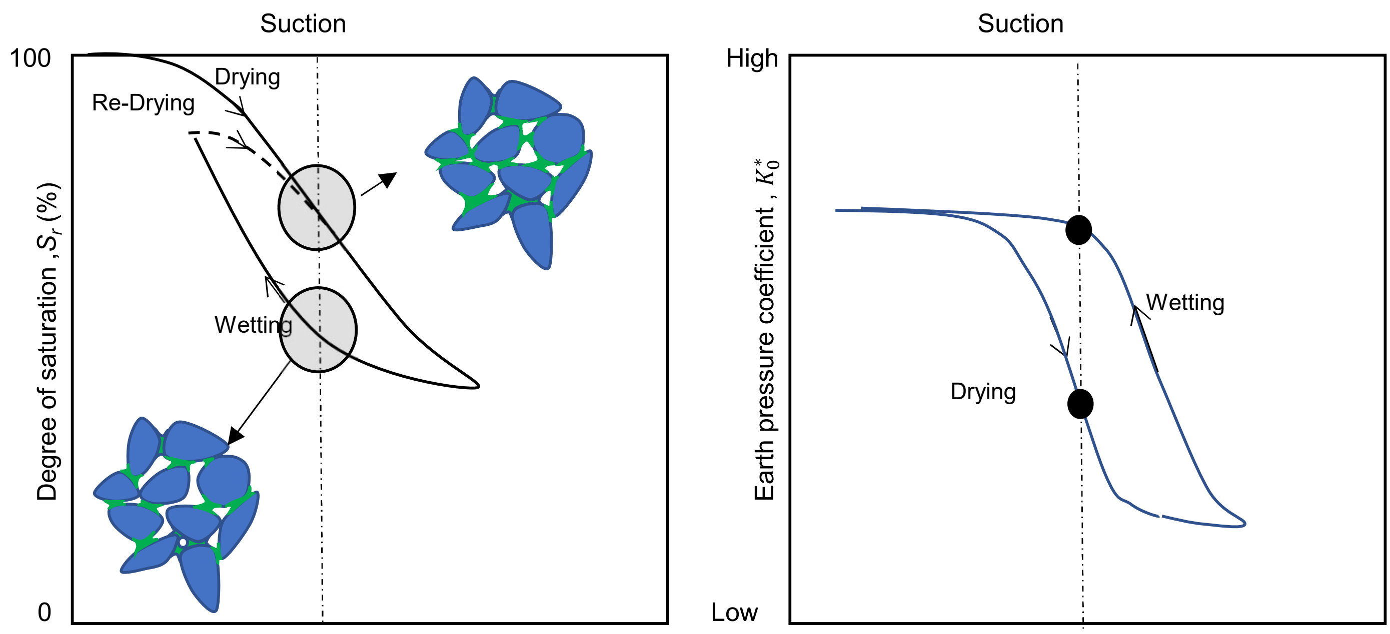

(a): A typical SWRC for soils

(b): K_0^* variations during wetting and drying

Figure 20 SWRC and K_0^* variations during wetting and drying